Manuscript Details

Manuscript number	EST_2019_217_R1
Title	Study of the influence of particle size of activate carbon for the manufacture of electrodes for supercapacitors
Article type	Research Paper

Abstract

By a mechanical treatment of ball milling and from a commercial activate carbon (CAC), four different samples, with different particle size between 200 nm and 1,3 mm, were obtained. These samples were chemically, texturally and morphologically characterized. Likewise, the influence of the particle size on the electrical qualities of the electrodes made for supercapacitors were studied. It was shown that milling process improves, in all cases, the electrical qualities of the supercapacitor made with original CAC. Nevertheless, it was observed that, from a certain particle size, due to particle agglomeration, the electrical capacity of supercapacitors decreased. Carbon black Vulcan 3 (V3) was used as mesoporous additive in order to improve the electrical capacities. The electrical capacity of the samples studied increased between 6 and 221 %, in most cases, when V3 was used. In addition, we modelled and printed in 3D, the central parts of the supercapacitors used in this study.

Keywords	Supercapacitors; energy storage; 3D printing; particle size; electrodes
Taxonomy	Energy, Chemical Energy Storage

Corresponding Author	Antonio Macias García
Order of Authors	Antonio Macias García, Diego Torrejón-Martín, M. Ángeles Díaz-Díez, Juan Pablo Carrasco Amador

Suggested reviewers	Paulo Brito, Rafael Balart, Ricardo Caruso

Submission Files Included in this PDF

File Name [File Type]

Cover Letter.pdf [Cover Letter]

Detailed Response to Reviewers_EST_2019_217.docx [Response to Reviewers]

Manuscript_revised_310519.docx [Revised Manuscript with Changes Marked]

Highlights.pdf [Highlights]

Manuscript_250319.docx [Manuscript File]

Fig1_Adsorption isotherms.jpg [Figure]

Fig2_DFT Method.jpg [Figure]

Fig3_BJH Method.jpg [Figure]

Figure4_new.jpg [Figure]

Fig5_Electrical conductivity.jpg [Figure]

Fig6_Electrical capacity 0.5V w-o V3.jpg [Figure]

Fig7_Electrical capacity 0.5V V3.jpg [Figure]

Fig8_Voltages comparison GMI 1240.jpg [Figure]

Fig9_Voltages comparison GMI 1240-10.jpg [Figure]

Fig10_Voltages comparison GMI 1240-30.jpg [Figure]

Fig11_Voltages comparison GMI 1240-120.jpg [Figure]

To view all the submission files, including those not included in the PDF, click on the manuscript title on your EVISE Homepage, then click 'Download zip file'.

Antonio Macías García, PhD
School of Industrial Engineering
University of Extremadura
Avda. de Elvas, s/n.
06006. Badajoz (Spain)
amacgar@unex.es

March 14, 2019

General Editor
JOURNAL OF ENERGY STORAGE

Dear Editor,

Please find enclosed the manuscript entitled *"Study of the influence of particle size of activate carbon for the manufacture of electrodes for supercapacitors"* for consideration to be published in *Journal of Energy Storage*.

The work has not been published previously and it is not under consideration for publication elsewhere. Its publication is approved by all authors and, if accepted, it will not be published elsewhere including electronically in the same form, in English or in any other language, without the written consent of the copyright- holder.

If you need any further information, please do not hesitate to contact me again at your convenience.

I look forward to hearing from you soon.

Best regards,

Antonio Macías-García, PhD

University of Extremadura

Antonio Macías-García, Ph.D
School of Industrial Engineering
University of Extremadura
Avda. de Elvas, s/n.
06006. Badajoz (Spain)
amacgar@unex.es

May 31, 2019

General Editor
JOURNAL OF ENERGY STORAGE

RESPONSE TO REVIEWERS:

Dear Editor,

We appreciate the comments made, as they suppose contributions that undoubtedly, clarify and greatly improve the text and interest of this article.
I attach the entire revised article, indicating in blue the contributions and changes for the manuscript entitled: "*Study of the influence of particle size of activated carbon for the manufacture of electrodes for supercapacitors*".

Reviewer 1:

1. In the abstract it is mentioned that "in addition, we have modeled and printed in 3D, the central parts of the supercapacitors used in this study" but there is not any information in the work on this aspect; should be complemented.

The information in the article has been completed. The central part of the Swagelok cell was designed with Inventor® CAD software that allows mechanical design and 3D simulation and then printed in 3D using fused filament fabrication.

2.- the introduction of the work is vague and does not present the state of the art of the use of these electrodes and should therefore be completed;

The “introduction” has been expanded and improved.

3.- A more complete carbon granulometric distribution should be presented after the grinding process;

Particle size information is given in Table 3. Particle size distribution is difficult to evaluate due to sample agglomeration problems (see SEM).

Antonio Macías-García, Ph.D
School of Industrial Engineering
University of Extremadura
Avda. de Elvas, s/n.
06006. Badajoz (Spain)
amacgar@unex.es

4.- Considering the influence of the pressure on the electrical conductivity of the material (as shown in the results, figure 5) it is believed that there should be an explanation for using a pressure of 100 bar in the production of the electrodes;

The discussion of the results obtained and shown in figure 5 has been expanded and improved.

100 bar pressure in the fabrication process of all electrodes increased electrical conductivity and compaction, which favors the electrode does not fall apart in the presence of electrolyte.

5.- Since the surface area is one of the most important parameters in the capacitors, and the production process of the electrodes can influence the final area of the electrodes, it is considered very relevant for the discussion of the results obtained the information of electrodes BET surface areas after its construction should be presented; it is effectively suspected that this is the aspect that justifies the observed behavior;

The electrodes have been manufactured with carbon blacks and PVDF in smaller proportion. Therefore, it was considered that as the activated carbon was in a higher proportion and given that the proportion of carbon black was constant, the possible variation of the BET surface of the prepared samples was the same for all.

6.- the conclusions should be reviewed in order to be more general.

The "conclusions" section has been revised, completed and improved.

Reviewer 2:

1.- The paper aims to investigate the effect of particle size of active carbon for the manufacture of électrodes for supercapacitors. The comments are given below:
- Authors should write the Nomenclature.

Added in the text:

GMI-1240 is commercial activated carbon.

GMI-1240- t, are the carbons resulting from the grinding time (10, 30 120 min).

Antonio Macías-García, Ph.D
School of Industrial Engineering
University of Extremadura
Avda. de Elvas, s/n.
06006. Badajoz (Spain)
amacgar@unex.es

2.- The following points should be addressed in the text

-The calibration processus for each apparatus? What is the uncertainty range for each experiment? the reproducibility of each experiment ?

Added in the text.

Each apparatus was previously calibrated, using standard patterns.

What makes high reproducibility possible.

Reviewer 3:

1.- The manuscript “Study of the influence of particle size of activate carbon for the manufacture of electrodes for supercapacitors” shows interesting results in its field. The manuscript is well structured and in general, the comments are well supported by the experimental data. The title is consistent with the content. Discussion is clear, well presented and supported by data and references. Conclusions are well supported by data. Nevertheless, some changes must be addressed by the authors for further consideration.

In English, decimal separators are usually points, not commas. Please, the authors must be review all text, including figures and tables, and change this.

Corrected in the text.

2.- In “Materials and methods” section, the equipment model, manufacturer, etc. of the SEM in page 3; Is the same that of page 4? Please, indicate this.

More detail and explanation has been included in the article.

Added on page 3: Scanning electron microscopy Hitachi Microscope S-4800.

3.- Please, in general consider the appropriate and uniform number of decimals that provide meaningful information (see for example Table 3).

Corrected in the Table 3.

4.- In page 5, last paragraph, Table 1 must be Table 4. Review this.

Corrected in the text. Table 4.

Antonio Macías-García, Ph.D
School of Industrial Engineering
University of Extremadura
Avda. de Elvas, s/n.
06006. Badajoz (Spain)
amacgar@unex.es

5.- In Table 4, check “0,.095” value.

Corrected in the Table 4.

6.- For the FT-IR analysis, I recommend showing a graph. It help to follow the discussion.

The initial sample is GMI 1.240 and the rest of the samples have only experienced a physical milling treatment, therefore their chemical composition does not change. Therefore, the FT-IR spectrum of GMI 1.240 is not enclosed in the article. The FT-IR spectrum of the GMI1.240 sample does not provide more data than the peaks already discussed in the article.

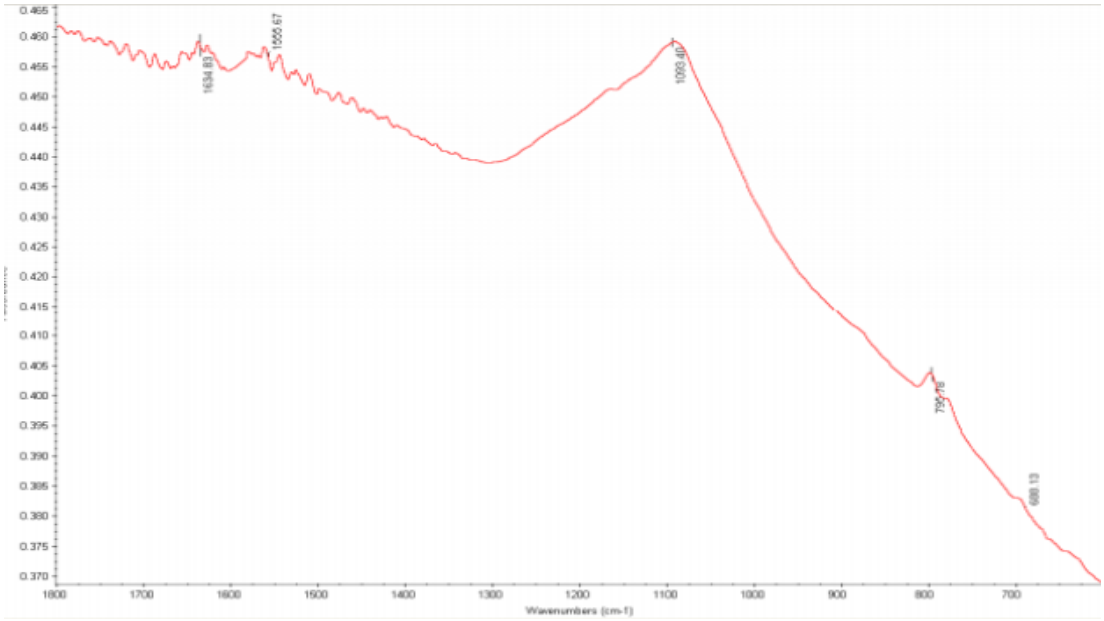

7.- The quality of the SEM images is low. It must be improved.

Corrected.

A new image of better quality is provided.

Antonio Macías-García, Ph.D
School of Industrial Engineering
University of Extremadura
Avda. de Elvas, s/n.
06006. Badajoz (Spain)
amacgar@unex.es

8.- In “3.5. Conductivity” section is said that “The results shown in the table …”; In what table?

Corrected in the text .

It has been specified in the article: “The results shown in the figure 5 reveal that as the grinding time increases (smaller particle sizes), the conductivity decreases”.

9.- The authors say that they have modelled and printed in 3D the central parts of the supercapacitors used in this study. It would be appropriate give more information regarding this and show some photograph.

The information in the article has been completed.

The central part of the Swagelok cell was designed with Inventor® CAD software that allows mechanical design and 3D simulation and then printed in 3D sing fused filament fabrication.

10.- Reference [28] is missing in the text. Please review references.

Corrected.

I look forward to hearing from you soon.

Best regards,

Antonio Macías-García, Ph.D

University of Extremadura

Study of the influence of particle size of activate carbon for the manufacture of electrodes for supercapacitors

Antonio Macías-García[1*], Diego Torrejón-Martín[1],
Mª Ángeles Díaz-Díez[1], Juan Pablo Carrasco-Amador[2]

[1]*Deparment of Mechanical, Energetic and Materials Engineering. School of industrial Engineering. University of Extremadura. Avda. de Elvas, s/n, 06006, Badajoz. Spain*
[2]*Deparment of Graphic Expression. School of industrial Engineering. University of Extremadura. Avda. de Elvas, s/n, 06006, Badajoz. Spain*

Abstract

By a mechanical treatment of ball milling and from a commercial activate carbon (CAC), four different samples, with different particle size between 200 nm and 1,3 mm, were obtained. These samples were chemically, texturally and morphologically characterized. Likewise, the influence of the particle size on the electrical qualities of the electrodes made for supercapacitors were studied. It was shown that milling process improves, in all cases, the electrical qualities of the supercapacitor made with original CAC. Nevertheless, it was observed that, from a certain particle size, due to particle agglomeration, the electrical capacity of supercapacitors decreased. Carbon black Vulcan 3 (V3) was used as mesoporous additive in order to improve the electrical capacities. The electrical capacity of the samples studied increased between 6 and 221 %, in most cases, when V3 was used. In addition, we modelled and printed in 3D, the central parts of the supercapacitors used in this study.

Keywords: Supercapacitors, energy storage, 3D printing, particle size, electrodes.

*Corresponding author:
E-mail address: amacgar@unex.es (Antonio Macías- García)

1. Introduction

Nowadays, the study of energy still remains the center of academic research, as well as of the development of new techniques globally. The main reason is that the sources of fossil fuels are not inexhaustible [1], [2], but there are other factors, such as global warming, or the exponential growth of the world population, leading to the fact that the methods of energy storage acquire more importance than ever. Among the energy storage devices supercapacitors are one of the most interesting technologies. [3]

This article focuses on the manufacture of electrodes for electric double layer capacitors (EDLCs), whose main advantages are its fast loading and unloading processes, its ability to release large power peaks and its long service life (> 106 cycles) [4]. The EDLCs are used in numerous applications [4-9], among which the automotive in electric and hybrid vehicles are the most notable ones.

Carbon materials, including carbon nanotubes, activated carbon (AC) [10], graphite, carbon aerogels [11], carbon nanofibers [12], etc., have been extensively studied for the manufacture of supercapacitation electrodes due to their large specific surface area, high conductivity and chemical stability [13]. The specific surface and porosity are essential for their electrochemical performance in supercapacitors [14]. Thus, an adequate distribution of micro and mesoporous can improve the electrochemical performance of this type of materials [15].

One of the materials used to manufacture EDLCs are activated carbons (AC) [5]. AC have a high specific surface area, chemical stability, good conductivity, charge accumulation capacity at the electrode/electrolyte interface and low economic cost, compared to other materials used in electrode production [1], [5], [16]. ACs are obtained from coal, products from biomass, polymers, etc. [1], [17], [18].

In recent years, research in the field of nanocarbons, microcarbons, estructurated carbons have increased, due to their excellent physical and chemical qualities [19], [20]. Thus, more and more researchers use nanoparticles and microparticles in the manufacture of carbon electrodes for supercapacitors. [21]

The disadvantage of these materials is the need to develop methods for large-scale manufacturing, to be fast and cost-effective, without altering their exceptional properties.

The objective of this work is to reduce the particle size of a commercial activated carbon to the nanometric or micrometric scale and to study its influence in the manufacture of electrodes for supercapacitors.

2. Materials and methods

2.1. Materials

Commercial activated carbon (CAC) GMI 1.240-1/S provided by CPL GalaQuim Ltd was used for the manufacture of the electrodes. Carbon black Vulcan 3 (V3) supplied by Carbot was employed in order to improve the conductivity of the electrodes manufactured, and polyvinylidene fluoride (PVDF) from the company Aldrich was used as a binding substance in the manufacture of the electrodes.

2.2. Procedure

The CAC was subjected to a mechanical treatment in a ball mill during different time periods (0, 10, 30 and 120 minutes), in order to reduce its particle size, generating the samples collected in table 1. The CAC milling was carried out in a SPEX SamplePrep 8000D Mixer / Mill® milled together with Tungsten carbide balls (WC) in a 1:10 ratio.

Sample	Milling time (min)
GMI 1.240	0
GMI 1.240-10	10
GMI 1.240-30	30
GMI 1.240-120	120

Table 1. Samples

GMI 1.240 is commercial activated carbon, GMI 1.240- t, are the carbons resulting from the grinding time (10, 30 and 120 min). The images corresponding to scanning electron microscopy Hitachi Microscope S-4800, were used to determine the particle size of the samples. For this purpose, the images were divided into 16 quadrants, and four of them, randomly chosen, were studied, as a way to obtain representative elements of the different particle sizes and their standard deviation in each sample.

The textural characterization of the samples was made from the adsorption isotherms of N_2 at -196 ˚C obtained by a QUANTACHROME AUTOSORB-1.

The electrical conductivity measurement (σ) was carried out in 0.08 g. sample, at room temperature by impedance spectroscopy in a frequency range of 20-10^6 Hz with a voltage of 1V on a Precision LCR Meter (QuadTech, model 1920).

Infrared spectroscopy with Fourier transform (FT-IR) was performed on a Perkin Elmer spectrometer, model 1720, between 400 and 4000 cm^{-1}.

The surface characterization of the samples was made by SEM, performed on a Hitachi Microscope S-4800, to study its morphology and agglomeration degree. From the characterized samples, eight electrodes, whose composition is shown in table 2, were manufactured.

	GMI 1240		GMI 1240-10		GMI 1240-30		GMI 1240-120	
	E1	E2	E3	E4	E5	E6	E7	E8
CA (%)	86.30	80.87	86.50	80.74	86.50	81.07	86.40	80.87
V3 (%)	0	5.68	0	5.68	0	5.55	0	5.68
PVDF (%)	13.70	13.45	13.50	13.58	13.50	13.38	13.60	13.45

Table 2. Electrodes composition

For the manufacture of the electrodes, the different components were mixed in an agate mortar. 0.1 g. of the total blend was taken and pressed into a titanium mold for 3 minutes, at 100 bar, in a CARVER uniaxial press model #3912. 100 bar pressure in the fabrication process of all prepared electrodes increases electrical conductivity and compaction.

Each apparatus was previously calibrated, using standard patterns.

The central part of the Swagelok cell was designed with Inventor® CAD software that allows mechanical design and 3D simulation and then printed in 3D using fused filament fabrication. Swagelok type electrochemical cells with configuration of two electrodes in the form of opposing discs have been used for the study of supercapacitors. The supercapacitors were formed by the aforementioned electrodes, an 0.5 M H_2SO_4 aqueous electrolyte, and glass fiber as a separating material. In order to study the behavior of the designed supercapacitors, both R and C were measured in a frequency range of 20-10^6 Hz, being examined at voltages of 0.2, 0.5 and 0.8 V. Precision LCR Meter (QuadTech, model 1920) measuring equipment was used.

3. Results and discussion

3.1. Mechanical treatment

The measured particle sizes are shown in table 3. As it can be seen in table 3, particle sizes vary between 1220 µm and 430 nm, in the micrometric-nanometric range.

Sample	Particle size		Standard deviation	
GMI 1.240	1220 µm		0.254	
GMI 1.240-10	2.040 µm	8.870 µm	0.660	7.210
GMI 1.240-30	0.610 µm	2.050 µm	0.200	0.830
GMI 1.240-120	0.430 µm	1.790 µm	0.200	0.670

Table 3. Particle sizes

As shown in figures 4 (a-d), as the milling time increases, the smaller particles (approximately 430 nm) undergo an agglomeration phenomenon around the larger particles, showing a heterogeneous distribution of particle size, and increasing intraparticle porosity.

3.2. Textural Characterization

From the adsorption isotherms of N_2 at -196 ° C (figure 1), the porous texture of the samples was determined. Their values are represented in table 4.

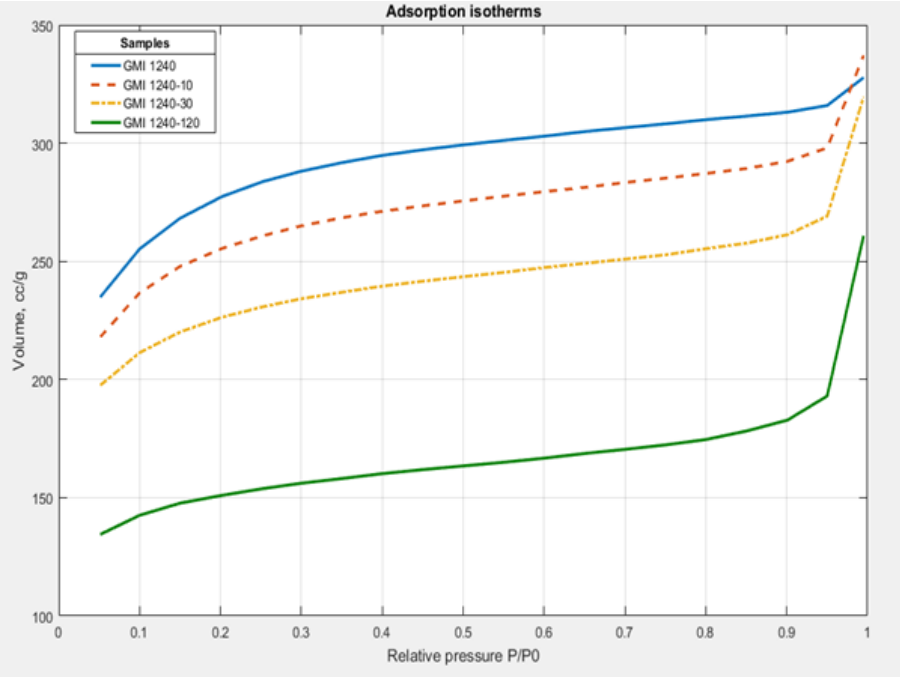

Figure 1. Adsorption isotherms of N_2 at -196˚C.

After having observed figure 1, the isotherms can be classified as type II isotherms, according to the BDDT classification [22]. All samples show an open elbow at low relative pressures, characteristic behavior of mesoporous solids. Likewise, the samples have a plateau with a slight upward slope at high relative pressures, characteristic behavior of the existence of mesoporous structures. Table 4 data shows that as the milling time increases, the BET surface of the samples decreases, GMI 1.240 > GMI 1.240-10 > GMI 1.240-30 > GMI 1.240-120. This fact can be explained by the destruction of part of the internal porous structure of the material in the milling. This table confirms that the samples are mainly microporous with a slight mesoporous development.

SAMPLE	SBET ($m^2 \cdot g^{-1}$)	Vmi ($cm^3 \cdot g^{-1}$)	Vme ($cm^3 \cdot g^{-1}$)
GMI 1.240	878.00	0.402	0.095
GMI 1.240-10	806.95	0.366	0.087
GMI 1.240-30	708.65	0.327	0.078
GMI 1.240-120	472.00	0.221	0.064

Table 4. Textural data of the samples

The pore size distribution was determinated by the DFT method (figure 2). Figure 2 shows that all the samples have a unimodal distribution, in which the micropores of approximately 5 Å

predominate. This behavior agrees with the elbows observed in the adsorption isotherms (figure 1). Figure 3 contains the data provided by the BJH method to determine the distribution of narrow mesopores. As it has been shown, there is evidence of narrow mesopores (<30Å). The behavior was similar for all samples.

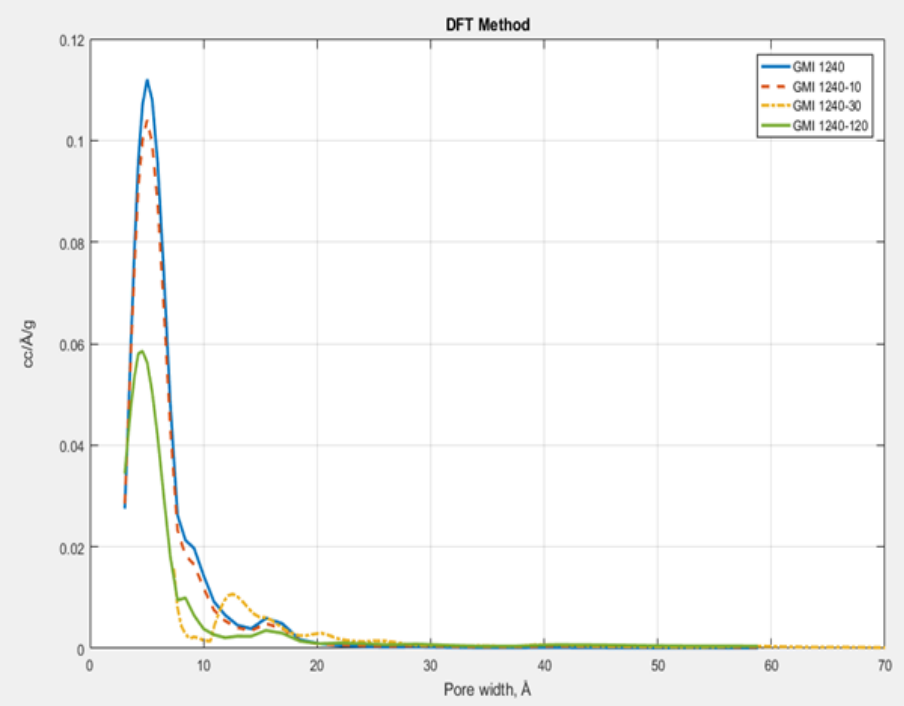

Figure 2. Pore size distribution by DFT method.

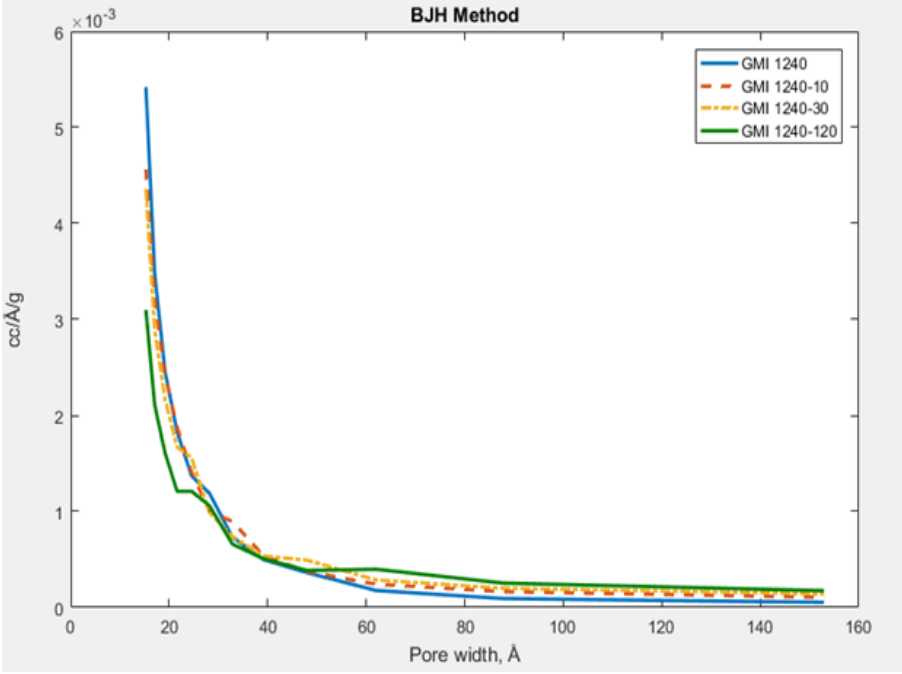

Figure 3. Narrow mesopore size distribution by BJH method.

3.3. Analysis of functional groups

The analysis of functional groups was performed only on the activated carbon GMI 1.240, since surface functional groups are not modified with mechanical treatment. The spectral range 1800-600 cm^{-1} has been represented as the range corresponding to the most interesting functional groups of an activated carbon. The band of approximately 1635 cm^{-1} corresponds to absorbed water that usually appears in the range of 1700 to 1600 cm^{-1}. The 1556 cm^{-1} band is attributed to the voltage vibration of the double bond C = C of aromatic rings, that usually appears in the range of 1600 to 1500 cm^{-1} with varying intensity. The 1093 cm^{-1} band is attributed to flexural vibrations in the plane of C-H bond of aromatic rings that give rise to absorptions between 1275 and 960 cm^{-1}. The 796 cm^{-1} and 688 cm^{-1} bands are attributed to out-of-plane flexion vibrations of the C-H bond of aromatic rings typically occurring in the range of 900-690 cm^{-1}.

3.4. Morphological analysis

The morphology of the samples has been studied by SEM (figures 4, a-d). They show how as the grinding time increases, the particle size decreases. The sizes obtained range from 1220 μm, of the unmilled sample (GMI 1.240), to particles of approximately 430 nm (GMI 1.240-120). It is also observed that in a same sample there is a heterogeneous distribution of particle size. This can be found in sample GMI 1.240-120, where a multitude of small particles (approximately 300 nm) coexist with larger particles (2500 nm). What causes a phenomenon of agglomeration of the smaller particles.

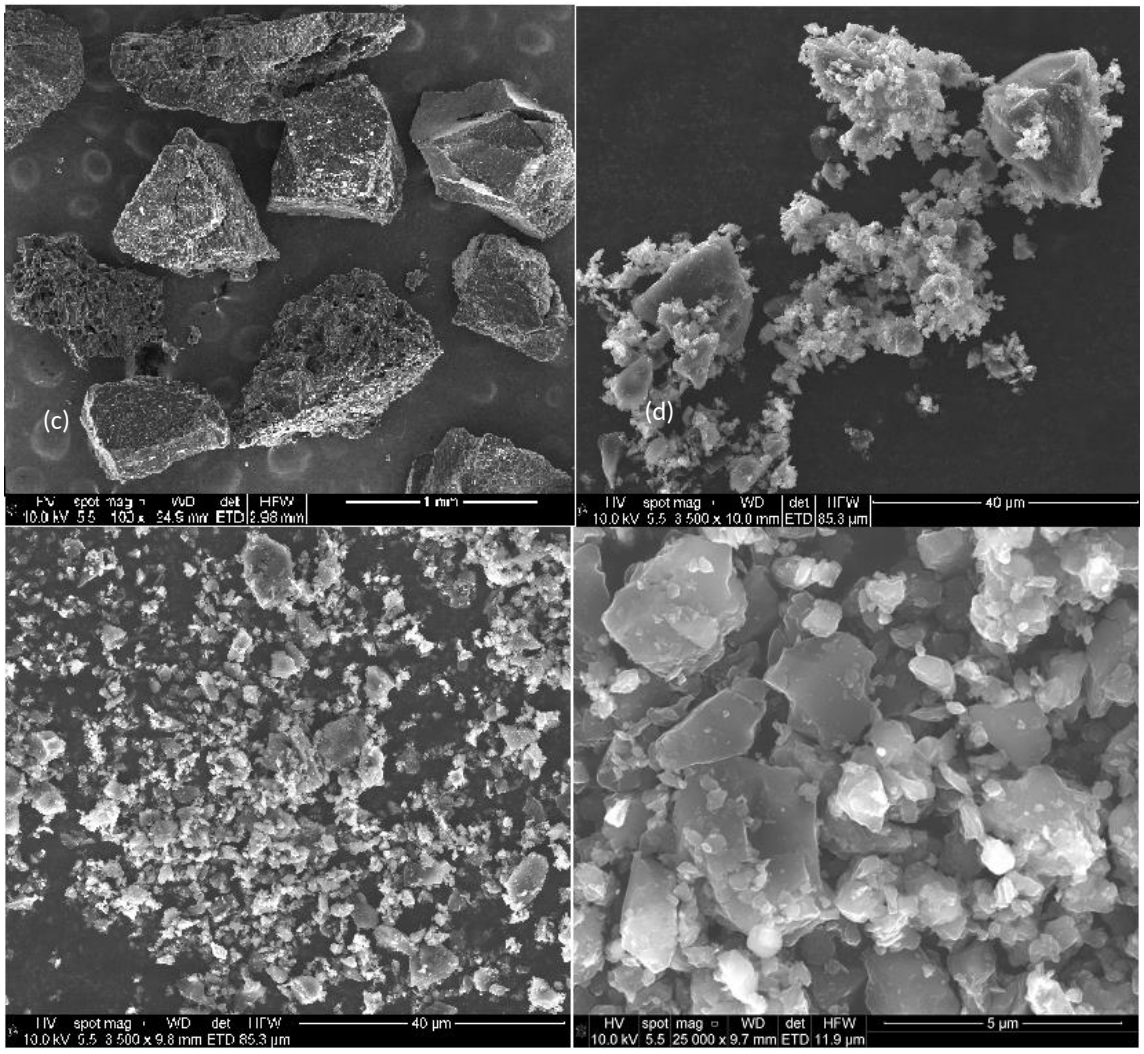

Figure 4. SEM of samples GMI 1.240 (a), GMI 1.240-10 (b), GMI 1.240-30 (c) and GMI 1.240-120 (d) respectively.

3.5. Conductivity

Figure 5 shows the variation of electrical conductivity of samples with the pressure, during the compaction process. The results shown in the figure 5 reveal that as the grinding time increases (smaller particle sizes), the conductivity decreases. This fact can be attributed to the increase of the intraparticle porosity, as seen in chapter 3.1. and as it is presented in the figures 4.

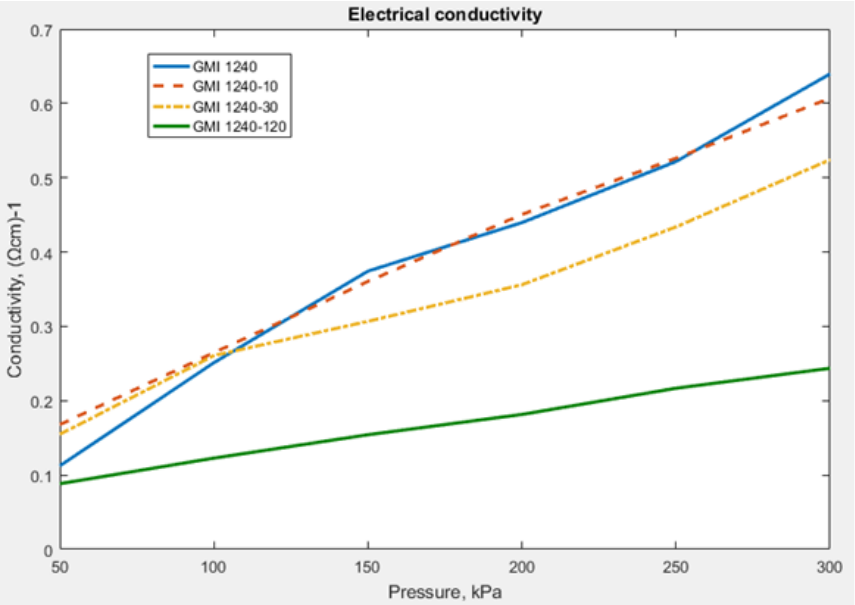

Figure 5. Electrical conductivity variation of the samples with the pressure during the compaction process.

For other researchers, the importance of mesoporous structure [23][24], chemical surface [25], physical and chemical properties [18-21], textural properties [27], etc., have a great influence on electrical properties of activated carbon.

3.6. Supercapacitors

In this chapter of the article, the study of prepared electrodes and their application to supercapacitors are addressed. For this purpose, we analize the influence of their composition, the electrolyte type and the concentration, and the voltage to which the different supercapacitors are subjected.

The Activated Carbons are materials of great interest to be used as electrodes in supercapacitors, due to their physical and chemical qualities combination, wich were detailed addressed in the introduction of this article.

The cell voltage is determined by the electrochemical stability of the electrolyte used. For aqueous electrolytes, the work potential cannot be higher than 1 V, because above that value electrolysis takes place. Aqueous electrolytes usually present a higher ionic conductivity, 0.8 S cm^{-1} for the H_2SO_4, versus lower values for organic electrolytes and a lower cost, from an economic point of view [28]. Other aspects to bear in mind when selecting an electrolyte are: the corrosive effects that can provoke the dissolution over the cell components, and the size of the ions solvating, as it can be happening that all the surface of the material of the electrode is

not accessible. The electrolyte concentration should be high enough to avoid its depletion. Already carried out research has shown that higher than 0.2M electrolyte concentrations are enough [29]. The supercapacitors resistance is highly influenced by the electrolyte resistivity and by the ions size that disseminate from the electrolyte to the pores of the electrode material. This does not mean a problem in the case of aqueous electrolytes as KOH or H_2SO_4, but it does, in the case of organic electrolytes, due to the higher size of their ions [30].

As for the study of the influence of the porous texture, because the first sample GMI 1.240, subjected to different milling processes and according to the figures 2 and 3, changes in its porous structure from the studies with DFT and BJH addressed in previous chapters are not observed. Nevertheless, some authors note that the sudden decrease in the specific capacity of activated carbons with the voltage is related to the samples microporosity, due to the slow diffusion of the ions to the pores [31], something that could justify the low capacity of the first sample GMI 1.240.

Study of the influence on carbon black and particle size

Two series of supercapacitors were carried away. The first one with V3 as a material providing mesopores, and the second one that only had CAC and PVDF. The measurement of supercapacitors electrical qualities was made as specified in the chapter 2.2.

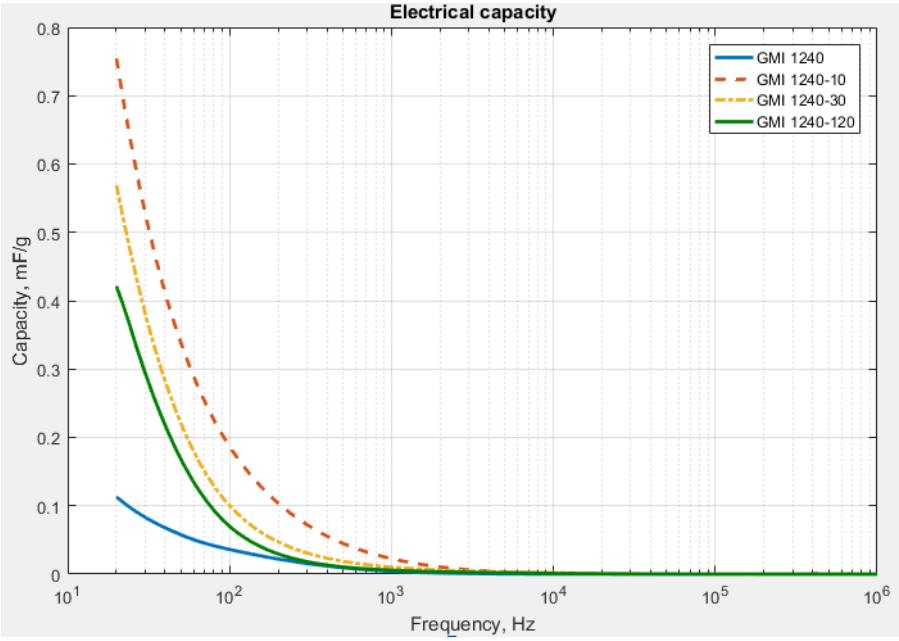

Figure 6. Samples not containing V3 in their composition tested at 0,5 V.

As seen in the figure 6, it can be observed that the milling improves the capacity of the original sample in approximately 569%, 405% and 273% (GMI 1.240-10, GMI 1.240-30 and GMI 1.240-120 samples respectively). However, after reaching a maximum, the capacity starts decreasing.

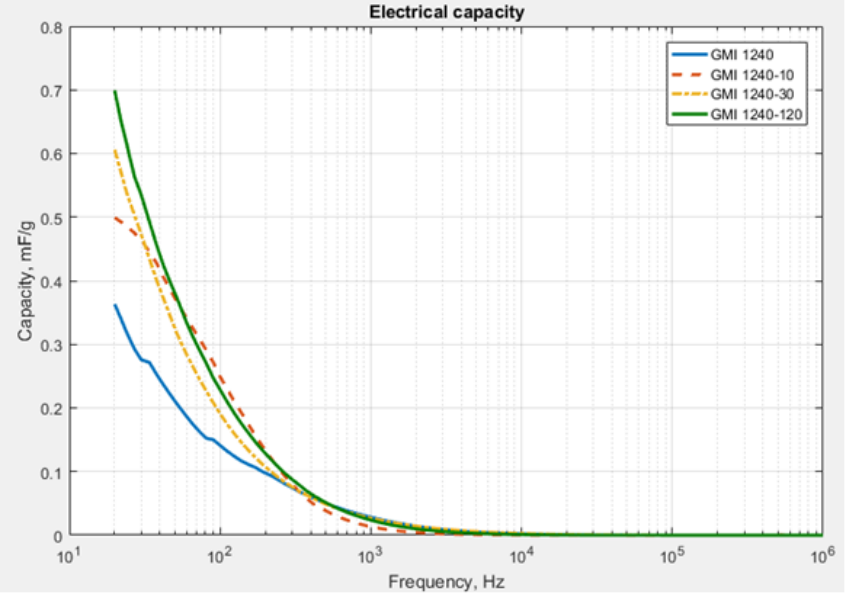

Figure 7. Samples containing V3 in their composition tested at 0,5 V.

The purpose of these two series (figures 6 and 7) is verifying if the presence of carbon black V3 in the electrodes composition, notably improves its electrical capacity. The possible improvement could be due to the fact that, structurally, carbon black V3 is mesoporous, in a way that favors a quick propagation of the charge in a brief period of time. This effect is clearly shown in the comparison of figures 6 and 7 where the samples GMI 1.240-120-V3 > GMI 1.240-120, GMI 1.240-30-V3 > GMI-1.240-30 y GMI-1.240-V3 > GMI 1.240 improve their electrical capacity in a 66.09%, 6.47% and 221.79% respectively.

However, in the sample GMI 1.240-10 V3 < GMI 1.240-10 the process reverses. This can be due to the fact that the particle size of the sample GMI-1.240-10 (2.04 μm – 8.87 μm) and of the V3, drastically reduce its superficial area, as well as its mechanical resistance. Finally, the percentage of carbon black present in the electrode, versus the particle size of the carbon black, is rendered in the fact that there is a higher number of repulsion electrostatic interactions that provoke that the electrode separated, deducting a considerable mechanical resistance and electrical capacity. Meanwhile in the rest of the samples it can be observed that the electrode presents a wide contact surface that allows a higher capacity of charge storing (figure 4). After having seen this effect, it remains crucial to reach a balance between the contribution of particle

size of activated carbon, and the quantity of activated carbon added to the electrode. Experimentally, it has been proved that adding carbon black in a proportion between the 5 and 6 % of the electrode mass, satisfies the balance between the increase of the electrical capacity and the loss of mechanical resistance in the electrode. This has allowed the development of stable and homogeneous electrodes, that present the desired behavior, as they are introduced within the fold of the electrolyte dissolution [32].

On the other hand, both series present a similar behavior, having higher electric capacity values at low frequencies, as it is shown in figures 6 and 7. In order to know the influence of voltage in electrical capacity, a measurement of the capacity of each sample at voltage 0.2, 0.5 and 0.8 V has been carried out, as shown in the figures 8-11.

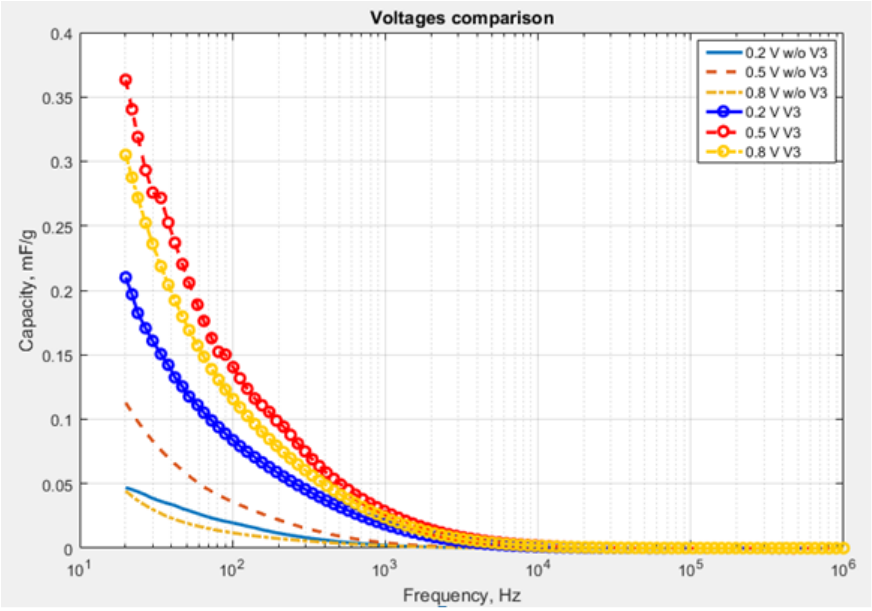

Figure 8. Comparison of GMI 1.240 samples not containing V3 and containing V3 at 0,2, 0,5 and 0,8 V.

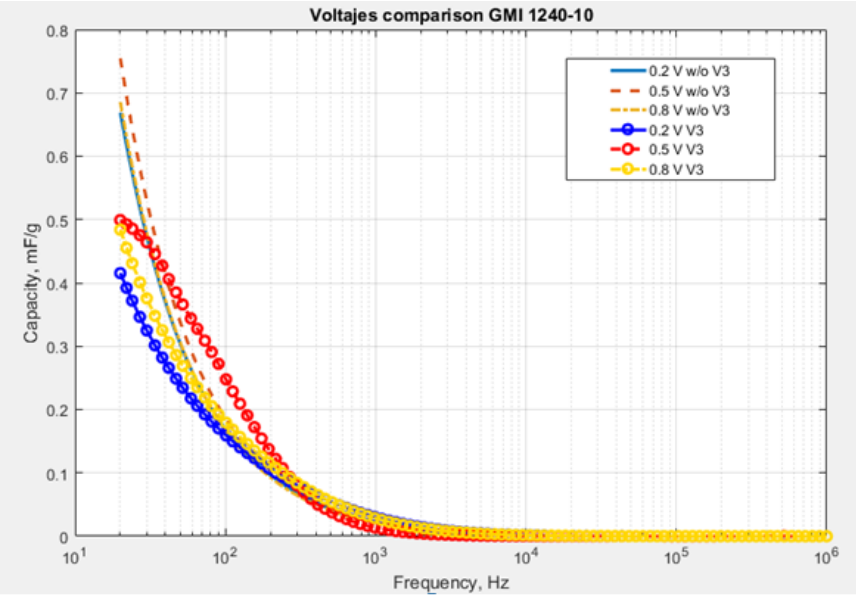

289

290 **Figure 9.** Comparison of GMI 1.240-10 samples not containing V3

291 and containing V3 at 0.2, 0.5 and 0.8 V.

292

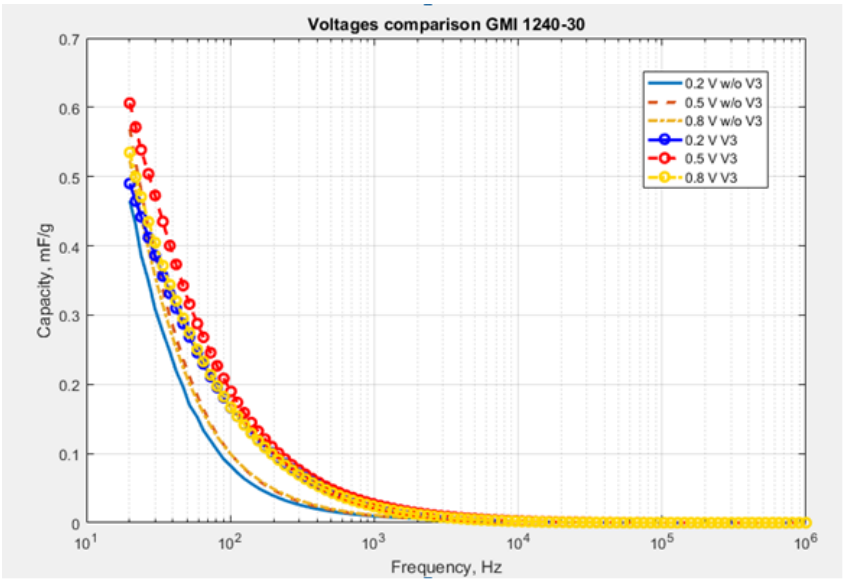

293

294 **Figure 10.** Comparison of GMI 1.240-30 samples not containing V3

295 and containing V3 at 0.2, 0.5 and 0.8 V.

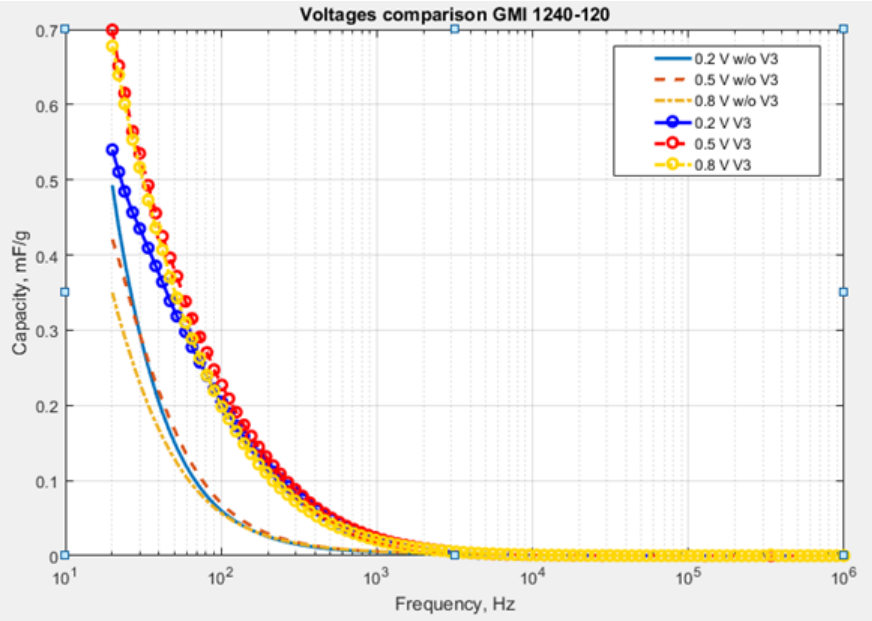

Figure 11. Comparison of GMI 1.240-120 samples not containing V3 and containing V3 at 0.2, 0.5 and 0.8 V.

Having seen figures from 8 to 11, it is clearly observed that prepared samples, both with V3 and without it, present a higher electrical capacity for 0.5 V voltage. This process can be due to the fact that voltage favors a better dissociation of the electrolyte and, in this way, facilitates the diffusion of the ions to the surface and to the pores of the samples that are object of this study. At low potentials of 0.2V, this dissociation process of sulfuric acid occurs with a lower intensity, something that explains the low results of the electrical capacity of the sample, as the mobility of the ions is reduced.

On the other hand, it can be expected that at 0.8V voltages, the supercapacitors electrical capacity was higher. However, it is not the case, and this can be because of a possible competition among the ions to occupy the active centers between the ions coming from the sulfuric acid, and the ones originated from the possible starting of the water electrolysis.

4. Conclusions

In short, with this article it has been proved that the increase of the supercapacitor capacity not only depends on the porosity, the pore distribution, the BET surface or the electrical conductivity, but also on the particle size, as the smaller particles see their surface increase and the contact among them benefits the electrical charge storage. The mechanical treatment to reduce the size particle, only exerts influence on the supercapacitor capacity in a limited amount of milling time (10 minutes), decreasing the capacity of supercapacitors for particle sizes

corresponding to longer milling periods and smaller sizes of particles, probably due to a particle agglomeration, and therefore decrease of the contact surface and increase of the interparticle porosity.

The milling of CAC improves the electrical capacity in all cases between a 273% and a 569%, as far as the GMI 1.240 is concerned, reaching a maximum after which the measurement that increases the milling time of the CA, decreases the supercapacitor capacity. The reason may be the agglomeration of the smaller particles as it is shown in figure 4. This fact can be solved with the addition of V3. Other authors that have used this technique to reduce the size particle, have experimented that the more the milling time, the lower the supercapacitor capacity [22-23],[34]. They believe that this fact is due to the mismatch produced in the size of the CA particles, as well to the additive used to improve its conductivity, and they solve it milling the additive together with the CA, something that can remain a new line of study for this project. The milling of the initial AC, V3 and PVDF could be a good solution to reduce the presence of a high interparticle porosity that affects the electrical capacity of the supercapacitor.

5. References

[1] Y. Huang *et al.*, "Sulfurized activated carbon for high energy density supercapacitors," *J. Power Sources*, vol. 252, pp. 90–97, 2014.

[2] T. Kousksou, P. Bruel, A. Jamil, T. El Rhafiki, and Y. Zeraouli, "Energy storage: Applications and challenges," *Sol. Energy Mater. Sol. Cells*, vol. 120, no. PART A, pp. 59–80, 2014.

[3] E. Miller, Y. Hua, and F. H. Tezel, "Materials for energy storage: Review of electrode materials and methods of increasing capacitance for supercapacitors," *J. Energy Storage*, vol. 20, pp. 30–40, Dec. 2018.

[4] Y. Qiu *et al.*, "Preparation of activated carbon paper through a simple method and application as a supercapacitor," *J. Mater. Sci.*, vol. 50, no. 4, pp. 1586–1593, 2015.

[5] J. Menzel, K. Fic, M. Meller, and E. Frackowiak, "The effect of halide ion concentration on capacitor performance," *J. Appl. Electrochem.*, pp. 1–7, 2014.

[6] D. Shin, K. Lee, and N. Chang, "Fuel economy analysis of fuel cell and supercapacitor hybrid systems," *Int. J. Hydrogen Energy*, vol. 41, no. 3, pp. 1381–1390, 2016.

[7] L. Chen, H. Yu, J. Zhong, L. Song, J. Wu, and W. Su, "Graphene field emitters : A review of fabrication , characterization and properties," vol. 220, pp. 44–58, 2017.

[8] L. Yingjian, Y. A. Abakr, Q. Qi, Y. Xinkui, and Z. Jiping, "Energy efficiency assessment of fixed asset investment projects - A case study of a Shenzhen combined-cycle power plant," *Renew. Sustain. Energy Rev.*, vol. 59, pp. 1195–1208, 2016.

[9] T. Ma, H. Yang, and L. Lu, "Development of hybrid battery-supercapacitor energy

storage for remote area renewable energy systems," *Appl. Energy*, vol. 153, pp. 56–62, 2015.

[10] S. Rawal, B. Joshi, and Y. Kumar, "Synthesis and characterization of activated carbon from the biomass of Saccharum bengalense for electrochemical supercapacitors," *J. Energy Storage*, vol. 20, pp. 418–426, Dec. 2018.

[11] U. Fischer, R. Saliger, V. Bock, R. Petricevic, "Carbon aerogels as electrode material in supercapacitors," *J Porous Mater*, vol. 4, no. 4, pp. 281–285, 1997.

[12] S. H. Yoon, S. Lim, Y. Song, Y. Ota, W. Qiao, A. Tanaka, "KOH activation of carbon nanofibers," *Carbon N. Y.*, vol. 42, no. 8–9, pp. 1723–1729, 2004.

[13] L.L. Zhang, "Carbon-based materials as supercapacitor electrodes," *Chem Soc Rev*, vol. 38, no. 9, pp. 2520–2531, 2009.

[14] C. Merino, P. Soto, E. Vilaplana-Ortego, J.M. Gomez de Salazar, F. Pico, "Carbon nanofibres and activated carbon nanofibres as electrodes in supercapacitors," *Carbon N. Y.*, vol. 43, no. 3, pp. 551–557, 2005.

[15] H. Chena, F. Wang, S. Tong, S. Guo, "Porous carbon with tailored pore size for electric double layer capacitors application," *Appl Surf Sci*, vol. 58, no. 16, pp. 6097–6102, 20112.

[16] C. H. Wang, W. C. Wen, H. C. Hsu, and B. Y. Yao, "High-capacitance KOH-activated nitrogen-containing porous carbon material from waste coffee grounds in supercapacitor," *Adv. Powder Technol.*, vol. 27, no. 4, pp. 1387–1395, 2016.

[17] F. Rodríguez-Reinoso and M. Molina-Sabio, "Activated carbons from lignocellulosic materials by chemical and/or physical activation: an overview," *Carbon N. Y.*, vol. 30, no. 7, pp. 1111–1118, 1992.

[18] A. B. Fuertes and M. Sevilla, "High-surface area carbons from renewable sources with a bimodal micro-mesoporosity for high-performance ionic liquid-based supercapacitors," *Carbon N. Y.*, vol. 94, pp. 41–52, 2015.

[19] L. S. S. et all Marisela Maubert F, "Nanotubos de Carbono - La era de la Nanotecnología," *Univ. Autónoma Metrop.*

[20] G. Tzvetkov, S. Mihaylova, K. Stoitchkova, P. Tzvetkov, and T. Spassov, "Mechanochemical and chemical activation of lignocellulosic material to prepare powdered activated carbons for adsorption applications," *Powder Technol.*, vol. 299, pp. 41–50, 2016.

[21] C. Niu, E. K. Sichel, R. Hoch, D. Moy, "High power electrochemical capacitors based on carbon nanotube electrodes," *Appl. Phys*, vol. 70, p. 1480, 1997.

[22] S. Brunauer, L. S. Deming, W. E. Deming, and E. Teller, "On a theory of the van der Waals adsorption of gases," *J. Am. Chem. Soc.*, vol. 62, no. 7, pp. 1723–1732, 1940.

[23] M. E. Ramos, P. R. Bonelli, and A. L. Cukierman, "Physico-chemical and electrical

properties of activated carbon cloths. Effect of inherent nature of the fabric precursor," *Colloids Surfaces A Physicochem. Eng. Asp.*, vol. 324, no. 1–3, pp. 86–92, 2008.

[24] V. Martín, M. J. Cocero, and S. Rodríguez-Rojo, "Fluidization of nanoparticles agglomerates enhanced by supercritical carbon dioxide," *Powder Technol.*, vol. 318, pp. 242–247, 2017.

[25] D. Pantea, H. Darmstadt, S. Kaliaguine, and C. Roy, "Electrical conductivity of conductive carbon blacks: Influence of surface chemistry and topology," *Appl. Surf. Sci.*, vol. 217, no. 1–4, pp. 181–193, 2003.

[26] D. L. Johnsen, Z. Zhang, H. Emamipour, Z. Yan, and M. J. Rood, "Effect of isobutane adsorption on the electrical resistivity of activated carbon fiber cloth with select physical and chemical properties," *Carbon N. Y.*, vol. 76, pp. 435–445, 2014.

[27] K. S.- Kumar, G. Vázquez, and A. Rodríguez, "Microwave Assisted Synthesis and Characterizations of Decorated Activated Carbon," vol. 7, pp. 5484–5494, 2012.

[28] V. Khomenko, E. Raymundo-Piñero, and F. Béguin, "Optimisation of an asymmetric manganese oxide/activated carbon capacitor working at 2 v in aqueous medium," *J. Power Sources*, vol. 153, no. 1, pp. 183–190, 2006.

[29] Zheng;Jow, "Effect of of Salt Salt Concentration in Electrolytes," *J. Electrochem. Soc.*, pp. 9–12, 1997.

[30] A. Burke, "Ultracapacitors: Why, how, and where is the technology," *J. Power Sources*, vol. 91, no. 1, pp. 37–50, 2000.

[31] B. E. Conway and W. G. Pell, "Power limitations of supercapacitor operation associated with resistance and capacitance distribution in porous electrode devices," *J. Power Sources*, vol. 105, no. 2, pp. 169–181, 2002.

[32] Cristina Gaya Jurado, "Fabricación de electrodos a pa," *Univ. Rey Juan Carlos*, p. 100790, 2009.

[33] L. S. Godse, P. B. Karandikar, and M. Y. Khaladkar, "Study of carbon materials and effect of its ball milling, on capacitance of supercapacitor," *Energy Procedia*, vol. 54, pp. 302–309, 2014.

[34] M. Ghaedi, S. Heidarpour, S. Nasiri Kokhdan, R. Sahraie, A. Daneshfar, and B. Brazesh, "Comparison of silver and palladium nanoparticles loaded on activated carbon for efficient removal of Methylene blue: Kinetic and isotherm study of removal process," *Powder Technol.*, vol. 228, pp. 18–25, 2012.

Table headings

Table 1. Samples

Table 2. Electrodes composition

Table 3. Particle sizes

Table 4. Textural data of the samples

Figure captions

Figure 1. Adsorption isotherms of N2 at -196˚C.

Figure 2. Pore size distribution by DFT method.

Figure 3. Narrow mesopore size distribution by BJH method.

Figure 4. SEM of samples GMI 1.240 (a), GMI 1.240-10 (b), GMI 1.240-30 (c) and GMI 1.240-120 (d) respectively.

Figure 5. Electrical conductivity variation of the samples with the pressure during the compaction process.

Figure 6. Samples not containing V3 in their composition tested at 0,5 V.

Figure 7. Samples containing V3 in their composition tested at 0,5 V.

Figure 8. Comparison of GMI 1.240 samples not containing V3 and containing V3 at 0,.2, 0,5 and 0,8 V.

Figure 9. Comparison of GMI 1.240-10 samples not containing V3 and containing V3 at 0,2, 0,5 and 0,8 V.

Figure 10. Comparison of GMI 1.240-30 samples not containing V3 and containing V3 at 0,2, 0,5 and 0,8 V.

Figure 11. Comparison of GMI 1.240-120 samples not containing V3 and containing V3 at 0,2, 0,5 and 0,8 V.

Antonio Macías García, PhD
School of Industrial Engineering
University of Extremadura
Avda. de Elvas, s/n.
06006. Badajoz (Spain)
amacgar@unex.es

March 14, 2019

General Editor
JOURNAL OF ENERGY STORAGE

Highlights:

- The increase of the capacity of the supercapacitors depends on the particle size.
- When the smaller particles increase, the storage of electrical charge increase.
- Reduce the size particle only exerts influence in a limited amount of milling time.
- Above that time, with smaller particle sizes, the capacity decreases.

Best regards,

Antonio Macías-García, PhD

University of Extremadura

Study of the influence of particle size of activate carbon for the manufacture of electrodes for supercapacitors

Antonio Macías-García[1*], Diego Torrejón-Martín[1],
Mª Ángeles Díaz-Díez[1], Juan Pablo Carrasco-Amador[2]

[1]*Deparment of Mechanical, Energetic and Materials Engineering. School of industrial Engineering. University of Extremadura. Avda. de Elvas, s/n, 06006, Badajoz. Spain*
[2]*Deparment of Graphic Expression. School of industrial Engineering. University of Extremadura. Avda. de Elvas, s/n, 06006, Badajoz. Spain*

Abstract

By a mechanical treatment of ball milling and from a commercial activate carbon (CAC), four different samples, with different particle size between 200 nm and 1,3 mm, were obtained. These samples were chemically, texturally and morphologically characterized. Likewise, the influence of the particle size on the electrical qualities of the electrodes made for supercapacitors were studied. It was shown that milling process improves, in all cases, the electrical qualities of the supercapacitor made with original CAC. Nevertheless, it was observed that, from a certain particle size, due to particle agglomeration, the electrical capacity of supercapacitors decreased. Carbon black Vulcan 3 (V3) was used as mesoporous additive in order to improve the electrical capacities. The electrical capacity of the samples studied increased between 6 and 221 %, in most cases, when V3 was used. In addition, we modelled and printed in 3D, the central parts of the supercapacitors used in this study.

Keywords: Supercapacitors, energy storage, 3D printing, particle size, electrodes.

*Corresponding author:
E-mail address: amacgar@unex.es (Antonio Macías- García)

1. Introduction

Nowadays, the study of energy still remains the center of academic research, as well as of the development of new techniques globally. The main reason is that the sources of fossil fuels are not inexhaustible [1], [2], but there are other factors, such as global warming, or the exponential growth of the world population, leading to the fact that the methods of energy storage acquire more importance than ever. Among the energy storage devices supercapacitors are one of the most interesting technologies.

This article focuses on the manufacture of electrodes for electric double layer capacitors (EDLCs), whose main advantages are its fast loading and unloading processes, its ability to release large power peaks and its long service life (> 106 cycles) [3]. The EDLCs are used in numerous applications [4-8], among which the automotive in electric and hybrid vehicles are the most notable ones.

One of the materials used to manufacture EDLCs are activated carbons (AC) [4]. AC have a high specific surface area, chemical stability, good conductivity, charge accumulation capacity at the electrode/electrolyte interface and low economic cost, compared to other materials used in electrode production [1], [4], [9]. ACs are obtained from coal, products from biomass, polymers, etc. [1], [10], [11].

In recent years, research in the field of nanocarbons has increased, due to their excellent physical and chemical qualities [12], [13]. The disadvantage of these materials is the need to develop methods for large-scale manufacturing, to be fast and cost-effective, without altering their exceptional properties.

The objective of this work is to reduce the particle size of a commercial activated carbon to the nanometric scale and to study its influence in the manufacture of electrodes for supercapacitors.

2. Materials and methods

2.1. Materials

Commercial activated carbon (CAC) GMI 1240-1/S provided by CPL GalaQuim Ltd was used for the manufacture of the electrodes. Carbon black Vulcan 3 (V3) supplied by Carbot was employed in order to improve the conductivity of the electrodes manufactured, and polyvinylidene fluoride (PVDF) from the company Aldrich was used as a binding substance in the manufacture of the electrodes.

2.2. Procedure

The CAC was subjected to a mechanical treatment in a ball mill during different time periods (0, 10, 30 and 120 minutes), in order to reduce its particle size, generating the samples collected in table 1. The CAC milling was carried out in a SPEX SamplePrep 8000D Mixer / Mill® milled together with Tungsten carbide balls (WC) in a 1:10 ratio.

Sample	Milling time (min)
GMI 1.240	0
GMI 1.240-10	10
GMI 1.240-30	30
GMI 1.240-120	120

Table 1. Samples

The images corresponding to scanning electron microscopy (SEM) were used to determine the particle size of the samples. For this purpose, the images were divided into 16 quadrants, and four of them, randomly chosen, were studied, as a way to obtain representative elements of the different particle sizes and their standard deviation in each sample.

The textural characterization of the samples was made from the adsorption isotherms of N2 at -196 ˚C obtained by a QUANTACHROME AUTOSORB-1.

The electrical conductivity measurement (σ) was carried out in 0,08 g. sample, at room temperature by impedance spectroscopy in a frequency range of 20-10^6 Hz with a voltage of 1V on a Precision LCR Meter (QuadTech, model 1920).

Infrared spectroscopy with Fourier transform (FT-IR) was performed on a Perkin Elmer spectrometer, model 1720, between 400 and 4.000 cm^{-1}.

The surface characterization of the samples was made by SEM, performed on a Hitachi Microscope S-4800, to study its morphology and agglomeration degree. From the characterized samples, eight electrodes, whose composition is shown in table 2, were manufactured.

	GMI 1240		GMI 1240-10		GMI 1240-30		GMI 1240-120	
	E1	E2	E3	E4	E5	E6	E7	E8
CA (%)	86,30	80,87	86,50	80,74	86,50	81,07	86,40	80,87
V3 (%)	0	5,68	0	5,68	0	5,55	0	5,68
PVDF (%)	13,70	13,45	13,50	13,58	13,50	13,38	13,60	13,45

Table 2. Electrodes composition

For the manufacture of the electrodes, the different components were mixed in an agate mortar. 0,1 g. of the total blend was taken and pressed into a titanium mold for 3 minutes, at 100 bar, in a CARVER uniaxial press model #3912.

Swagelok type electrochemical cells with configuration of two electrodes in the form of opposing discs have been used for the study of supercapacitors. The supercapacitors were formed by the aforementioned electrodes, an 0,5 M H_2SO_4 aqueous electrolyte, and glass fiber as a separating material. In order to study the behavior of the designed supercapacitors, both R and C were measured in a frequency range of 20-10^6 Hz, being examined at voltages of 0,2, 0,5 and 0,8 V. Precision LCR Meter (QuadTech, model 1920) measuring equipment was used.

3. Results and discussion

3.1. Mechanical treatment

The measured particle sizes are shown in table 3. As it can be seen in table 3, particle sizes vary between 1200 µm and 430 nm, in the micrometric-nanometric range.

Sample	Particle size		Standard deviation	
GMI 1.240	1.220 µm		0,254	
GMI 1.230-10	2,04 µm	8,87 µm	0,66	7,21

GMI 1.240-30	0,610 µm	2.050 µm	0,2	0,83
GMI 1.240-120	0,430 µm	1.790 µm	0,20	0,67

Table 3. Particle sizes

As shown in figures 4 (a-d), as the milling time increases, the smaller particles (approximately 430 nm) undergo an agglomeration phenomenon around the larger particles, showing a heterogeneous distribution of particle size, and increasing intraparticle porosity.

3.2. Textural Characterization

From the adsorption isotherms of N2 at -196 ° C (figure 1), the porous texture of the samples was determined. Their values are represented in table 4.

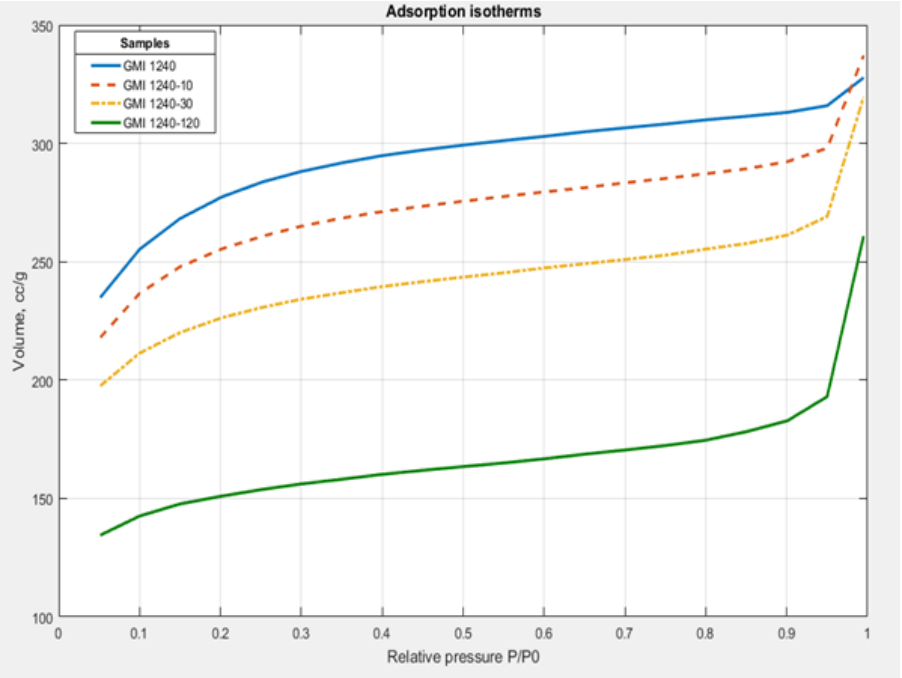

Figure 1. Adsorption isotherms of N2 at -196˚C.

After having observed figure 1, the isotherms can be classified as type II isotherms, according to the BDDT classification [14]. All samples show an open elbow at low relative pressures, characteristic behavior of mesoporous solids. Likewise, the samples have a plateau with a slight upward slope at high relative pressures, characteristic behavior of the existence of mesoporous structures. Table 1 data shows that as the milling time increases, the BET surface of the samples decreases, GMI 1.240 > GMI 1.240-10 > GMI 1.240-30 > GMI 1.240-120. This fact can be explained by the destruction of part of the internal porous structure of the material in the milling.

This table confirms that the samples are mainly microporous with a slight mesoporous development.

SAMPLE	SBET ($m^2 \cdot g^{-1}$)	Vmi ($cm^3 \cdot g^{-1}$)	Vme ($cm^3 \cdot g^{-1}$)
GMI 1.240	878,00	0,402	0,.095
GMI 1.240-10	806,95	0,366	0,087
GMI 1.240-30	708,65	0,327	0,078
GMI 1.240-120	472,00	0,221	0,064

Table 4. Textural data of the samples

The pore size distribution was determinated by the DFT method (figure 2). Figure 2 shows that all the samples have a unimodal distribution, in which the micropores of approximately 5 Å predominate. This behavior agrees with the elbows observed in the adsorption isotherms (figure 1). Figure 3 contains the data provided by the BJH method to determine the distribution of narrow mesopores. As it has been shown, there is evidence of narrow mesopores (<30Å). The behavior was similar for all samples.

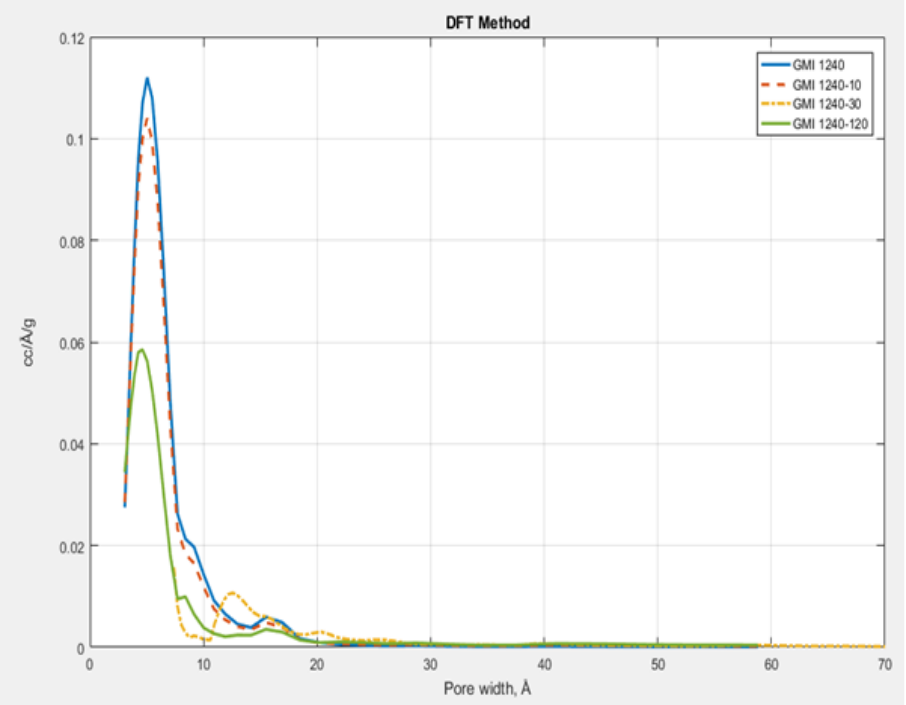

Figure 2. Pore size distribution by DFT method.

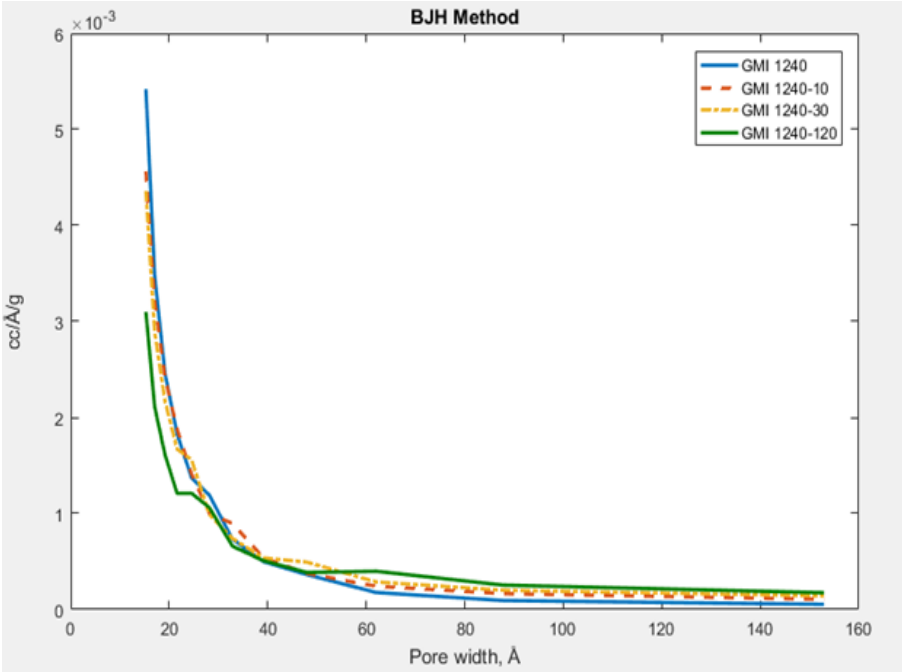

Figure 3. Narrow mesopore size distribution by BJH method.

3.3. Analysis of functional groups

The analysis of functional groups was performed only on the activated carbon GMI 1.240, since surface functional groups are not modified with mechanical treatment. The spectral range 1.800-600 cm^{-1} has been represented as the range corresponding to the most interesting functional groups of an activated carbon. The band of approximately 1.635 cm^{-1} corresponds to absorbed water that usually appears in the range of 1.700 to 1.600 cm^{-1}. The 1.556 cm^{-1} band is attributed to the voltage vibration of the double bond C = C of aromatic rings, that usually appears in the range of 1.600 to 1.500 cm^{-1} with varying intensity. The 1.093 cm^{-1} band is attributed to flexural vibrations in the plane of C-H bond of aromatic rings that give rise to absorptions between 1.275 and 960 cm^{-1}. The 796 cm^{-1} and 688 cm^{-1} bands are attributed to out-of-plane flexion vibrations of the C-H bond of aromatic rings typically occurring in the range of 900-690 cm^{-1}.

3.4. Morphological analysis

The morphology of the samples has been studied by SEM (figures 4, a-d). They show how as the grinding time increases, the particle size decreases. The sizes obtained range from 1.220 μm, of the unmilled sample (GMI 1.240), to particles of approximately 430 nm (GMI 1.240-120). It is also observed that in a same sample there is a heterogeneous distribution of particle size. This can be found in sample GMI 1.240-120, where a multitude of small particles (approximately 300 nm)

coexist with larger particles (2.500 nm). What causes a phenomenon of agglomeration of the smaller particles.

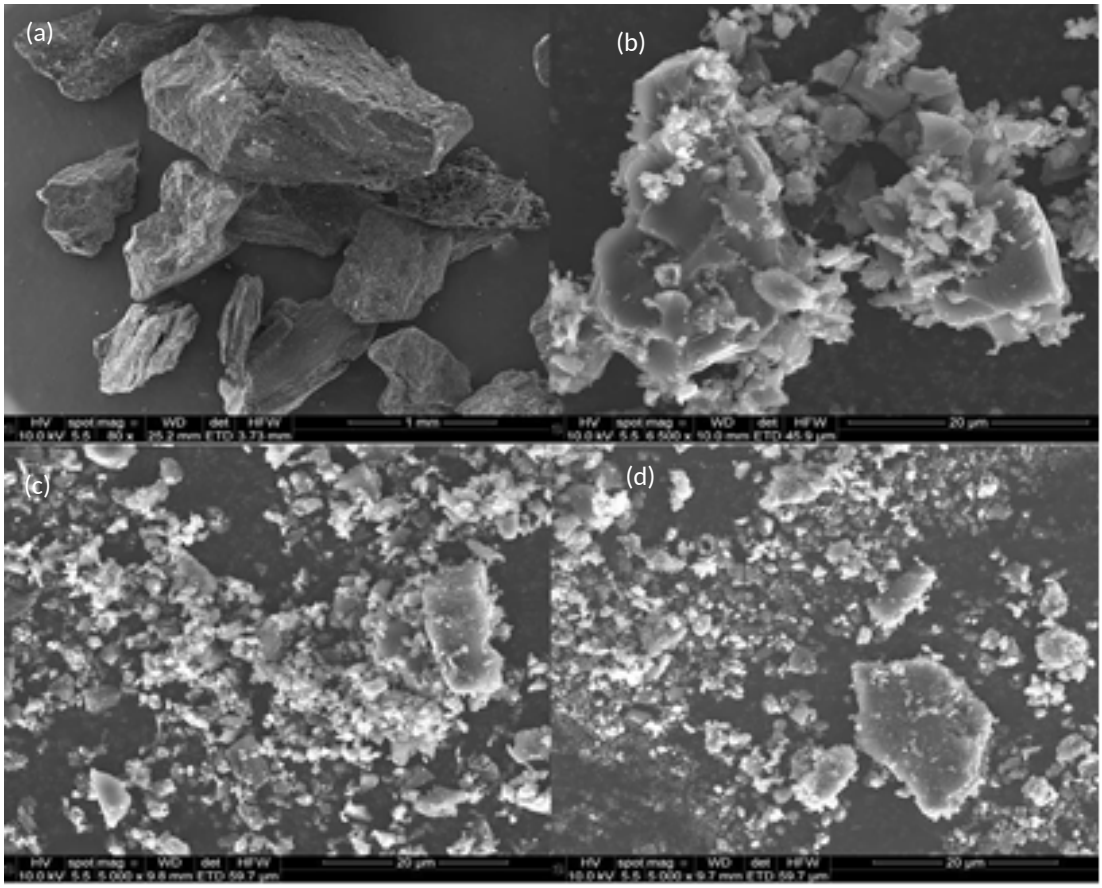

Figure 4. SEM of samples GMI 1.240 (a), GMI 1.240-10 (b), GMI 1.240-30 (c) and GMI 1.240-120 (d) respectively.

3.5. Conductivity

Figure 5 shows the variation of electrical conductivity of samples with the pressure, during the compaction process. The results shown in the table reveal that as the grinding time increases (smaller particle sizes), the conductivity decreases. This fact can be attributed to the increase of the intraparticle porosity, as seen in chapter 3.1. and as it is presented in the figures 4.

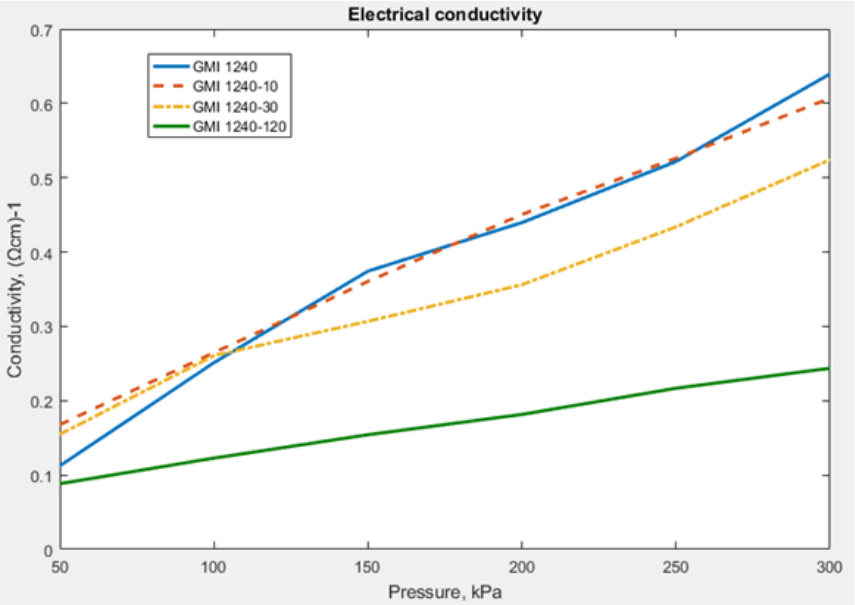

Figure 5. Electrical conductivity variation of the samples with the pressure during the compaction process.

For other researchers, the importance of mesoporous structure [15][16], chemical surface [17], physical and chemical properties [18-21], textural properties [22], etc., have a great influence on electrical properties of activated carbon.

3.6. Supercapacitors

In this chapter of the article, the study of prepared electrodes and their application to supercapacitors are addressed. For this purpose, we analize the influence of their composition, the electrolyte type and the concentration, and the voltage to which the different supercapacitors are subjected.

The Activated Carbons are materials of great interest to be used as electrodes in supercapacitors, due to their physical and chemical qualities combination, wich were detailed addressed in the introduction of this article.

The cell voltage is determined by the electrochemical stability of the electrolyte used. For aqueous electrolytes, the work potential cannot be higher than 1 V, because above that value electrolysis takes place. Aqueous electrolytes usually present a higher ionic conductivity, 0,8 S cm^{-1} for the H_2SO_4, versus lower values for organic electrolytes and a lower cost, from an economic point of view [23]. Other aspects to bear in mind when selecting an electrolyte are: the corrosive effects that can provoke the dissolution over the cell components, and the size of the ions solvating, as it can be happening that all the surface of the material of the electrode is not accessible. The

electrolyte concentration should be high enough to avoid its depletion. Already carried out research has shown that higher than O,2M electrolyte concentrations are enough [24]. The supercapacitors resistance is highly influenced by the electrolyte resistivity and by the ions size that disseminate from the electrolyte to the pores of the electrode material. This does not mean a problem in the case of aqueous electrolytes as KOH or H_2SO_4, but it does, in the case of organic electrolytes, due to the higher size of their ions [25].

As for the study of the influence of the porous texture, because the first sample GMI 1.240, subjected to different milling processes and according to the figures 2 and 3, changes in its porous structure from the studies with DFT and BJH addressed in previous chapters are not observed. Nevertheless, some authors note that the sudden decrease in the specific capacity of activated carbons with the voltage is related to the samples microporosity, due to the slow diffusion of the ions to the pores [26], something that could justify the low capacity of the first sample GMI 1.240.

Study of the influence on carbon black and particle size

Two series of supercapacitors were carried away. The first one with V3 as a material providing mesopores, and the second one that only had CAC and PVDF. The measurement of supercapacitors electrical qualities was made as specified in the chapter 2.2.

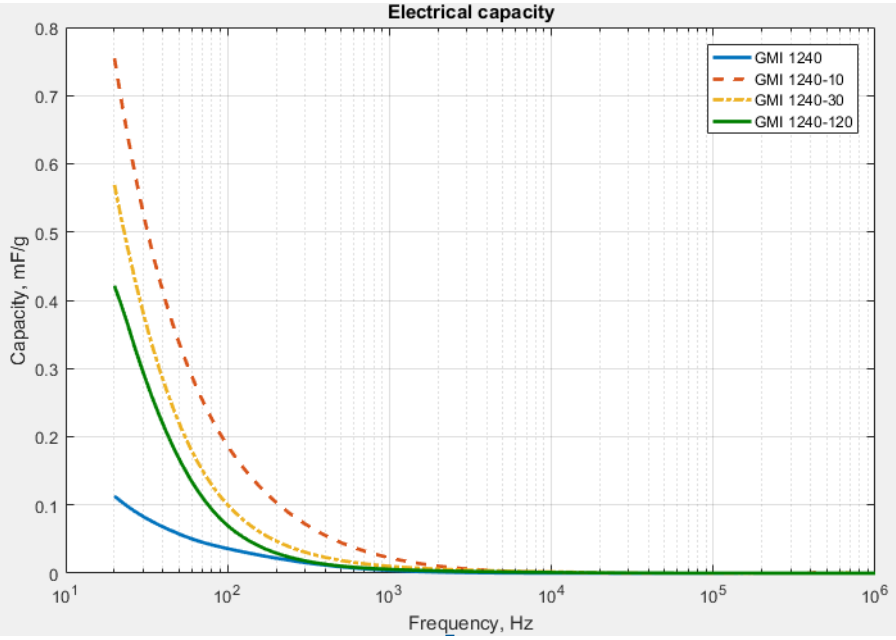

Figure 6. Samples not containing V3 in their composition tested at 0,5 V.

As seen in the figure 6, it can be observed that the milling improves the capacity of the original sample in approximately 569%, 405% and 273% (GMI 1.240-10, GMI 1.240-30 and GMI 1.240-120 samples respectively). However, after reaching a maximum, the capacity starts decreasing.

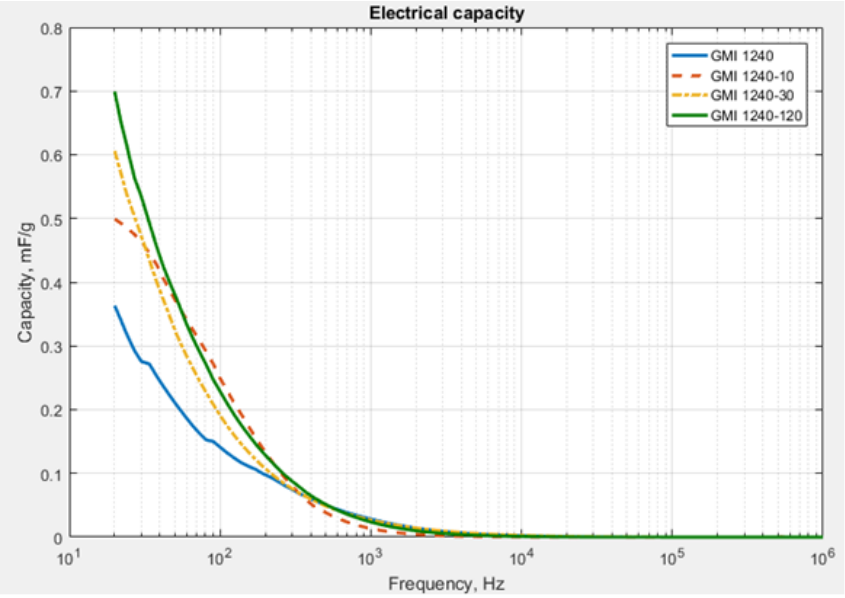

Figure 7. Samples containing V3 in their composition tested at 0,5 V.

The purpose of these two series (figures 6 and 7) is verifying if the presence of carbon black V3 in the electrodes composition, notably improves its electrical capacity. The possible improvement could be due to the fact that, structurally, carbon black V3 is mesoporous, in a way that favors a quick propagation of the charge in a brief period of time. This effect is clearly shown in the comparison of figures 6 and 7 where the samples GMI 1.240-120-V3 > GMI 1.240-120, GMI 1.240-30-V3 > GMI-1.240-30 y GMI-1.240-V3 > GMI 1.240 improve their electrical capacity in a 66,09%, 6,47% and 221,79% respectively.

However, in the sample GMI 1.240-10 V3 < GMI 1.240-10 the process reverses. This can be due to the fact that the particle size of the sample GMI-1.240-10 (2,04 µm – 8,87 µm) and of the V3, drastically reduce its superficial area, as well as its mechanical resistance. Finally, the percentage of carbon black present in the electrode, versus the particle size of the carbon black, is rendered in the fact that there is a higher number of repulsion electrostatic interactions that provoke that the electrode separated, deducting a considerable mechanical resistance and electrical capacity. Meanwhile in the rest of the samples it can be observed that the electrode presents a wide contact surface that allows a higher capacity of charge storing (figure 4). After having seen this effect, it remains crucial to reach a balance between the contribution of particle size of activated carbon, and the quantity of activated carbon added to the electrode. Experimentally, it has been proved

that adding carbon black in a proportion between the 5 and 6 % of the electrode mass, satisfies the balance between the increase of the electrical capacity and the loss of mechanical resistance in the electrode. This has allowed the development of stable and homogeneous electrodes, that present the desired behavior, as they are introduced within the fold of the electrolyte dissolution [27].

On the other hand, both series present a similar behavior, having higher electric capacity values at low frequencies, as it is shown in figures 6 and 7. In order to know the influence of voltage in electrical capacity, a measurement of the capacity of each sample at voltage 0,2, 0,5 and 0,8 V has been carried out, as shown in the figures 8-11.

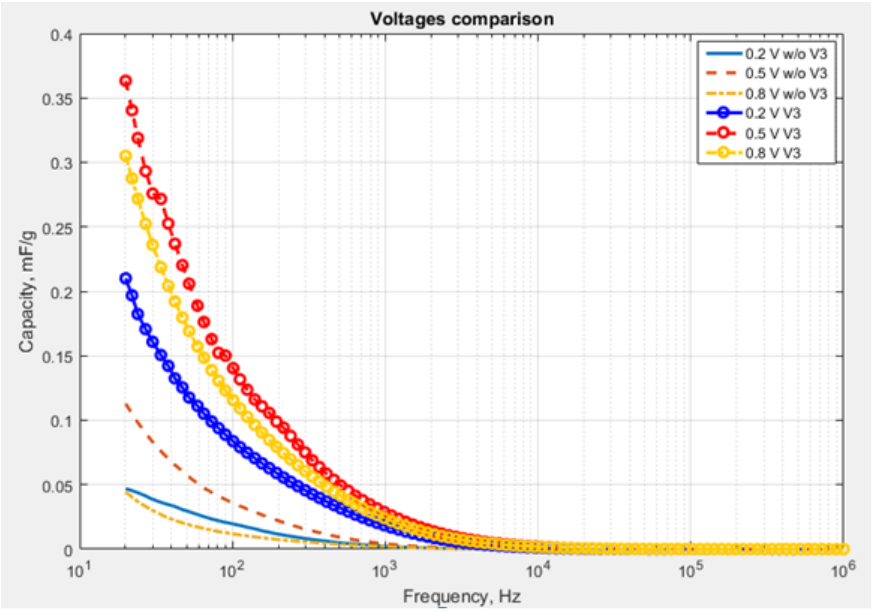

Figure 8. Comparison of GMI 1.240 samples not containing V3 and containing V3 at 0,2, 0,5 and 0,8 V.

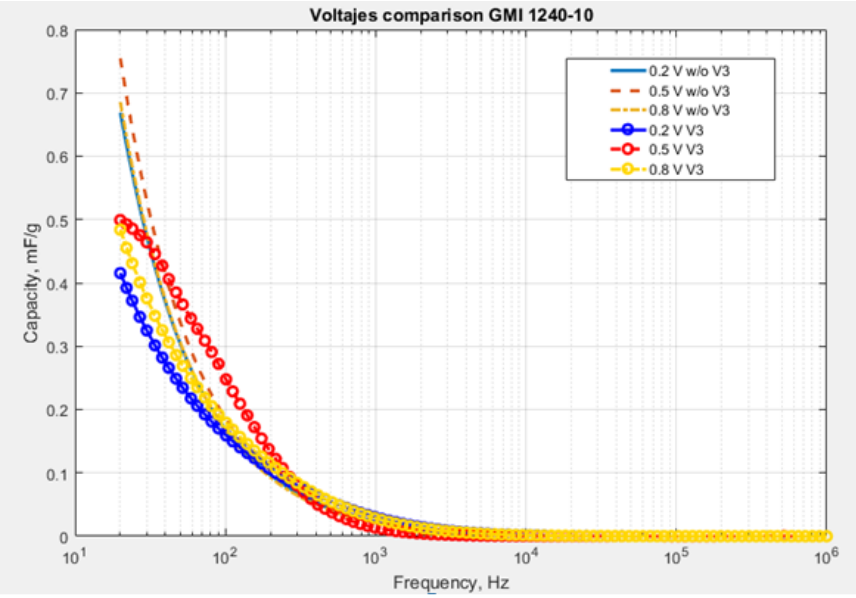

Figure 9. Comparison of GMI 1.240-10 samples not containing V3 and containing V3 at 0,2, 0,5 and 0,8 V.

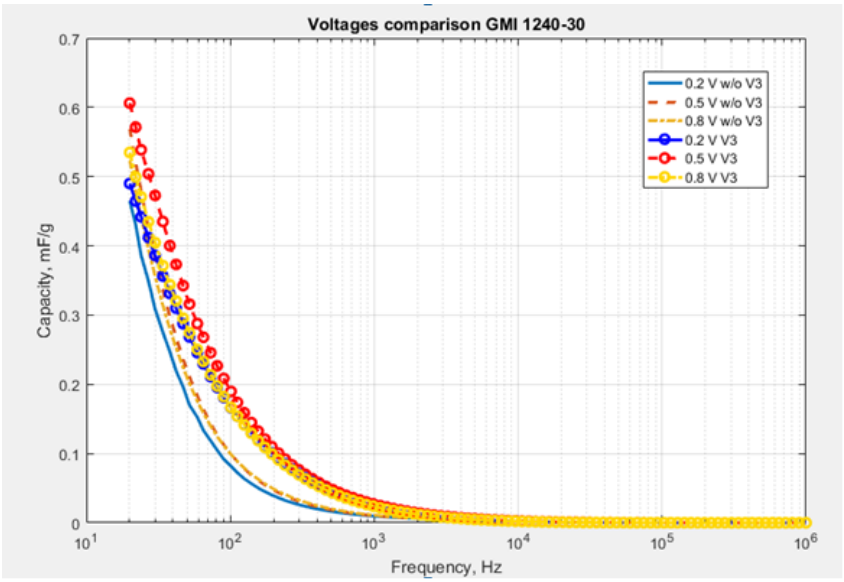

Figure 10. Comparison of GMI 1.240-30 samples not containing V3 and containing V3 at 0,.2, 0,5 and 0,8 V.

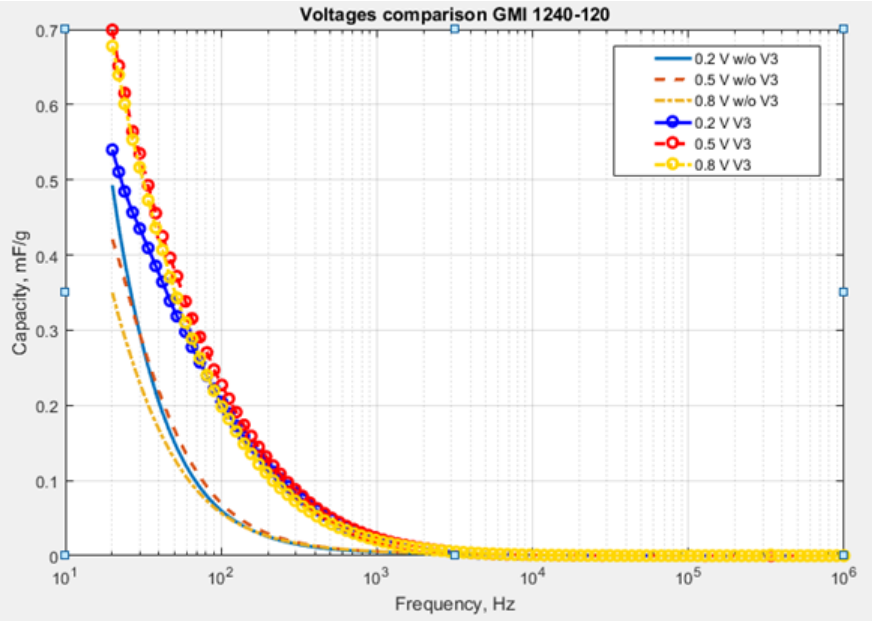

Figure 11. Comparison of GMI 1.240-120 samples not containing V3 and containing V3 at 0,2, 0,5 and 0,8 V.

Having seen figures from 8 to 11, it is clearly observed that prepared samples, both with V3 and without it, present a higher electrical capacity for 0,5 V voltage. This process can be due to the fact that voltage favors a better dissociation of the electrolyte and, in this way, facilitates the diffusion of the ions to the surface and to the pores of the samples that are object of this study. At low potentials of 0,2V, this dissociation process of sulfuric acid occurs with a lower intensity, something that explains the low results of the electrical capacity of the sample, as the mobility of the ions is reduced.

On the other hand, it can be expected that at 0,8V voltages, the supercapacitors electrical capacity was higher. However, it is not the case, and this can be because of a possible competition among the ions to occupy the active centers between the ions coming from the sulfuric acid, and the ones originated from the possible starting of the water electrolysis.

4. Conclusions

In short, with this article it has been proved that the increase of the supercapacitor capacity not only depends on the porosity, the pore distribution, or the electrical conductivity, but also on the particle size, as the smaller particles see their surface increase and the contact among them benefits the electrical charge storage. The mechanical treatment to reduce the size particle, only exerts influence on the supercapacitor capacity in a limited amount of milling time (10 minutes),

decreasing the capacity of supercapacitors for particle sizes corresponding to longer milling periods and smaller sizes of particles, probably due to a particle agglomeration.

The milling of CAC improves the electrical capacity in all cases between a 273% and a 569%, as far as the GMI 1.240 is concerned, reaching a maximum after which the measurement that increases the milling time of the CA, decreases the supercapacitor capacity. The reason may be the agglomeration of the smaller particles as it is shown in figure 4. This fact can be solved with the addition of V3. Other authors that have used this technique to reduce the size particle, have experimented that the more the milling time, the lower the supercapacitor capacity [22-23],[29]. They believe that this fact is due to the mismatch produced in the size of the CA particles, as well to the additive used to improve its conductivity, and they solve it milling the additive together with the CA, something that can remain a new line of study for this project.

5. References

[1] Y. Huang, S. L. Candelaria, Y. Li, Z. Li, J. Tian, L. Zhang, and G. Cao, "Sulfurized activated carbon for high energy density supercapacitors," *J. Power Sources*, vol. 252, pp. 90–97, 2014.

[2] T. Kousksou, P. Bruel, A. Jamil, T. El Rhafiki, and Y. Zeraouli, "Energy storage: Applications and challenges," *Sol. Energy Mater. Sol. Cells*, vol. 120, no. PART A, pp. 59–80, 2014.

[3] Y. Qiu, Z. Cheng, B. Guo, H. Fan, S. Sun, T. Wu, L. Jin, L. Fan, and X. Feng, "Preparation of activated carbon paper through a simple method and application as a supercapacitor," *J. Mater. Sci.*, vol. 50, no. 4, pp. 1586–1593, 2015.

[4] J. Menzel, K. Fic, M. Meller, and E. Frackowiak, "The effect of halide ion concentration on capacitor performance," *J. Appl. Electrochem.*, pp. 1–7, 2014.

[5] D. Shin, K. Lee, and N. Chang, "Fuel economy analysis of fuel cell and supercapacitor hybrid systems," *Int. J. Hydrogen Energy*, vol. 41, no. 3, pp. 1381–1390, 2016.

[6] L. Chen, H. Yu, J. Zhong, L. Song, J. Wu, and W. Su, "Graphene field emitters : A review of fabrication , characterization and properties," vol. 220, pp. 44–58, 2017.

[7] L. Yingjian, Y. A. Abakr, Q. Qi, Y. Xinkui, and Z. Jiping, "Energy efficiency assessment of fixed asset investment projects - A case study of a Shenzhen combined-cycle power plant," *Renew. Sustain. Energy Rev.*, vol. 59, pp. 1195–1208, 2016.

[8] T. Ma, H. Yang, and L. Lu, "Development of hybrid battery-supercapacitor energy storage for remote area renewable energy systems," *Appl. Energy*, vol. 153, pp. 56–62, 2015.

[9] C. H. Wang, W. C. Wen, H. C. Hsu, and B. Y. Yao, "High-capacitance KOH-activated nitrogen-containing porous carbon material from waste coffee grounds in supercapacitor," *Adv. Powder Technol.*, vol. 27, no. 4, pp. 1387–1395, 2016.

[10] F. Rodríguez-Reinoso and M. Molina-Sabio, "Activated carbons from lignocellulosic materials by chemical and/or physical activation: an overview," *Carbon N. Y.*, vol. 30, no. 7, pp. 1111–1118, 1992.

[11] A. B. Fuertes and M. Sevilla, "High-surface area carbons from renewable sources with a bimodal micro-mesoporosity for high-performance ionic liquid-based supercapacitors," *Carbon N. Y.*, vol. 94, pp. 41–52, 2015.

[12] Laura Soto S., Marisela Maubert F., Ana M. León C. and Jorge Flores M., "Nanotubos de Carbono - La era de la Nanotecnología," *Univ. Autónoma Metrop.*

[13] G. Tzvetkov, S. Mihaylova, K. Stoitchkova, P. Tzvetkov, and T. Spassov, "Mechanochemical and chemical activation of lignocellulosic material to prepare powdered activated carbons for adsorption applications," *Powder Technol.*, vol. 299, pp. 41–50, 2016.

[14] S. Brunauer, L. S. Deming, W. E. Deming, and E. Teller, "On a theory of the van der Waals adsorption of gases," *J. Am. Chem. Soc.*, vol. 62, no. 7, pp. 1723–1732, 1940.

[15] M. E. Ramos, P. R. Bonelli, and A. L. Cukierman, "Physico-chemical and electrical properties of activated carbon cloths. Effect of inherent nature of the fabric precursor," *Colloids Surfaces A Physicochem. Eng. Asp.*, vol. 324, no. 1–3, pp. 86–92, 2008.

[16] V. Martín, M. J. Cocero, and S. Rodríguez-Rojo, "Fluidization of nanoparticles agglomerates enhanced by supercritical carbon dioxide," *Powder Technol.*, vol. 318, pp. 242–247, 2017.

[17] D. Pantea, H. Darmstadt, S. Kaliaguine, and C. Roy, "Electrical conductivity of conductive carbon blacks: Influence of surface chemistry and topology," *Appl. Surf. Sci.*, vol. 217, no. 1–4, pp. 181–193, 2003.

[18] D. L. Johnsen, Z. Zhang, H. Emamipour, Z. Yan, and M. J. Rood, "Effect of isobutane adsorption on the electrical resistivity of activated carbon fiber cloth with select physical and chemical properties," *Carbon N. Y.*, vol. 76, pp. 435–445, 2014.

[19] J. Kazmierczak-Razna, P. Nowicki, and R. Pietrzak, "Characterization and application of bio-activated carbons prepared by direct activation of hay with the use of microwave radiation," *Powder Technol.*, vol. 319, pp. 302–312, 2017.

[20] P. Nowicki, J. Kazmierczak, and R. Pietrzak, "Comparison of physicochemical and sorption properties of activated carbons prepared by physical and chemical activation of cherry stones," *Powder Technol.*, vol. 269, pp. 312–319, 2014.

[21] M. Ghasemi, M. Zeinaly Khosroshahy, A. Bavand Abbasabadi, N. Ghasemi, H. Javadian, and M. Fattahi, "Microwave-assisted functionalization of Rosa Canina-L fruits activated carbon with tetraethylenepentamine and its adsorption behavior toward Ni(II) in aqueous solution: Kinetic, equilibrium and thermodynamic studies," *Powder Technol.*, vol. 274, pp. 362–371, 2015.

[22] K. S.- Kumar, G. Vázquez, and A. Rodríguez, "Microwave Assisted Synthesis and Characterizations of Decorated Activated Carbon," vol. 7, pp. 5484–5494, 2012.

[23] V. Khomenko, E. Raymundo-Piñero, and F. Béguin, "Optimisation of an asymmetric manganese oxide/activated carbon capacitor working at 2 v in aqueous medium," *J. Power Sources*, vol. 153, no. 1, pp. 183–190, 2006.

[24] Zheng;Jow, "Effect of of Salt Salt Concentration in Electrolytes," *J. Electrochem. Soc.*, pp. 9–12, 1997.

[25] A. Burke, "Ultracapacitors: Why, how, and where is the technology," *J. Power Sources*, vol. 91, no. 1, pp. 37–50, 2000.

[26] B. E. Conway and W. G. Pell, "Power limitations of supercapacitor operation associated with resistance and capacitance distribution in porous electrode devices," *J. Power Sources*, vol. 105, no. 2, pp. 169–181, 2002.

[27] Cristina Gaya Jurado, "Fabricación de electrodos a pa," *Univ. Rey Juan Carlos*, p. 100790, 2009.

[28] L. S. Godse, P. B. Karandikar, and M. Y. Khaladkar, "Study of carbon materials and effect of its ball milling, on capacitance of supercapacitor," *Energy Procedia*, vol. 54, pp. 302–309, 2014.

[29] M. Ghaedi, S. Heidarpour, S. Nasiri Kokhdan, R. Sahraie, A. Daneshfar, and B. Brazesh, "Comparison of silver and palladium nanoparticles loaded on activated carbon for efficient removal of Methylene blue: Kinetic and isotherm study of removal process," *Powder Technol.*, vol. 228, pp. 18–25, 2012.

Table headings

Table 1. Samples

Table 2. Electrodes composition

Table 3. Particle sizes

Table 4. Textural data of the samples

Figure captions

Figure 1. Adsorption isotherms of N2 at -196˚C.

Figure 2. Pore size distribution by DFT method.

Figure 3. Narrow mesopore size distribution by BJH method.

Figure 4. SEM of samples GMI 1.240 (a), GMI 1.240-10 (b), GMI 1.240-30 (c) and GMI 1.240-120 (d) respectively.

Figure 5. Electrical conductivity variation of the samples with the pressure during the compaction process.

Figure 6. Samples not containing V3 in their composition tested at 0,5 V.

Figure 7. Samples containing V3 in their composition tested at 0,5 V.

Figure 8. Comparison of GMI 1.240 samples not containing V3 and containing V3 at 0,.2, 0,5 and 0,8 V.

Figure 9. Comparison of GMI 1.240-10 samples not containing V3 and containing V3 at 0,2, 0,5 and 0,8 V.

Figure 10. Comparison of GMI 1.240-30 samples not containing V3 and containing V3 at 0,2, 0,5 and 0,8 V.

Figure 11. Comparison of GMI 1.240-120 samples not containing V3 and containing V3 at 0,2, 0,5 and 0,8 V.

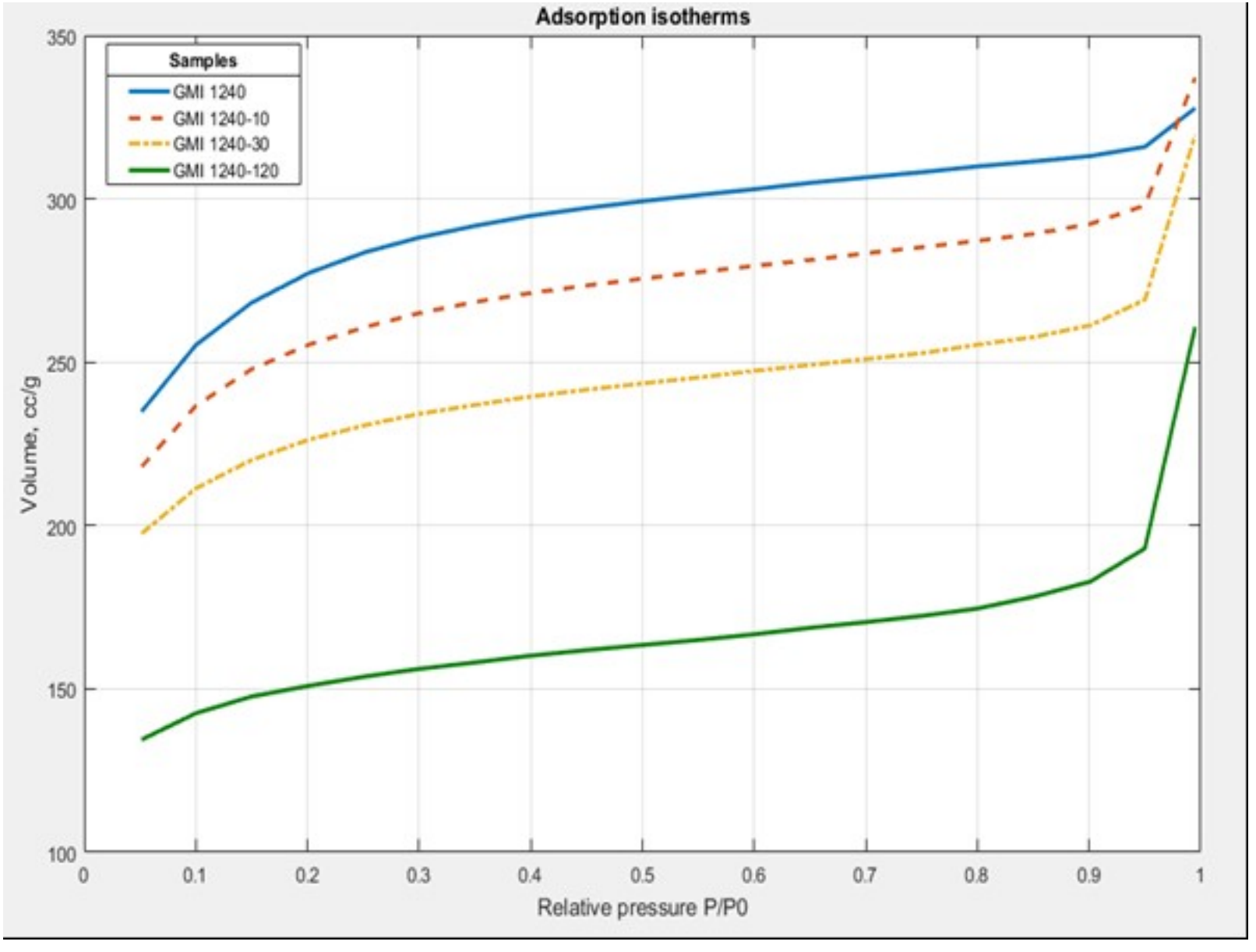
Adsorption isotherms
Samples
GMI 1240
GMI 1240-10
GMI 1240-30
GMI 1240-120
Volume, cc/g
Relative pressure P/P0
350
300
250
200
150
100
0
0.1
0.2
0.3
0.4
0.5
0.6
0.7
0.8
0.9
1

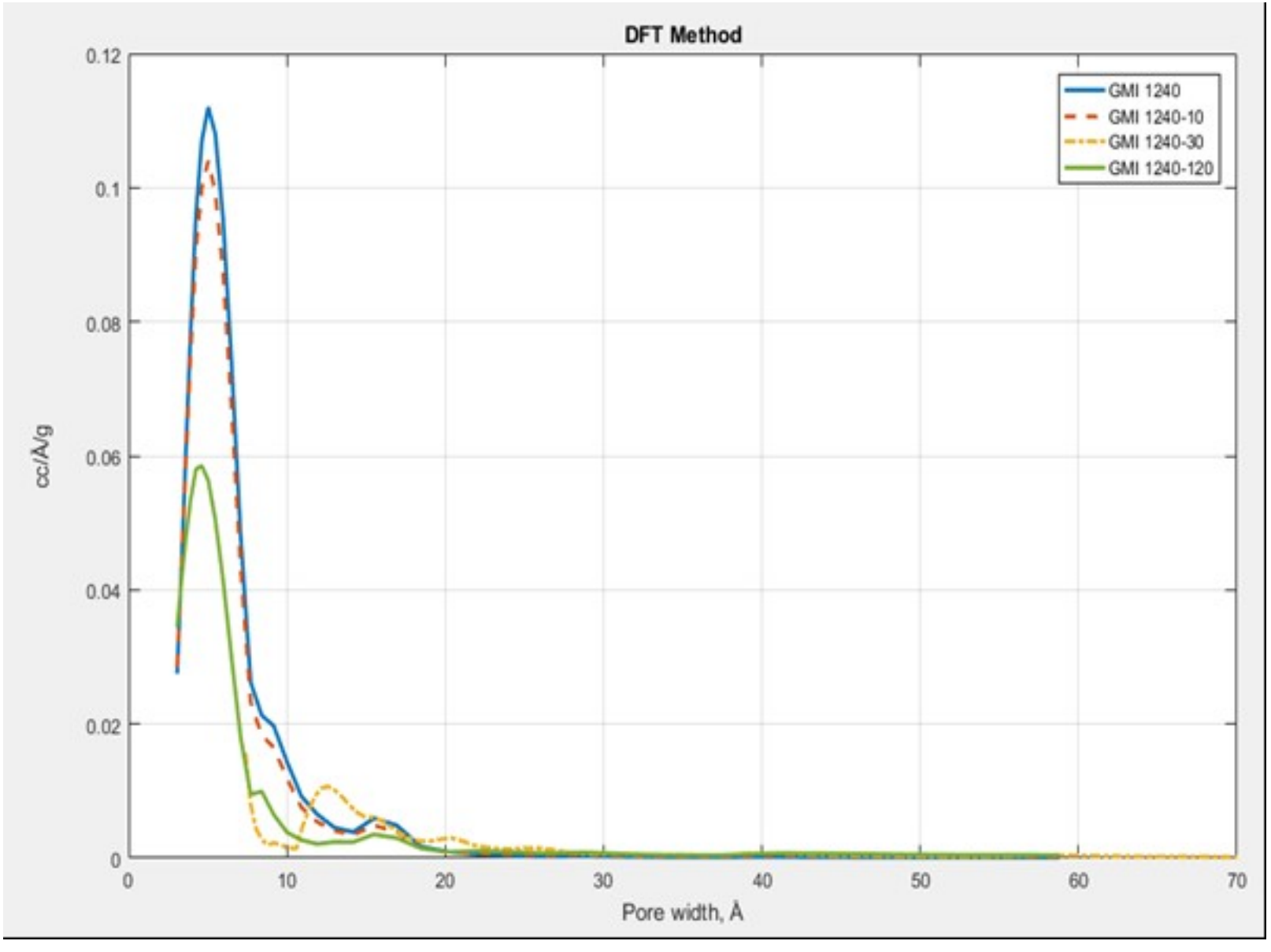
DFT Method
GMI 1240
GMI 1240-10
GMI 1240-30
GMI 1240-120
cc/Å/g
Pore width, Å
0.12
0.1
0.08
0.06
0.04
0.02
0
0
10
20
30
40
50
60
70

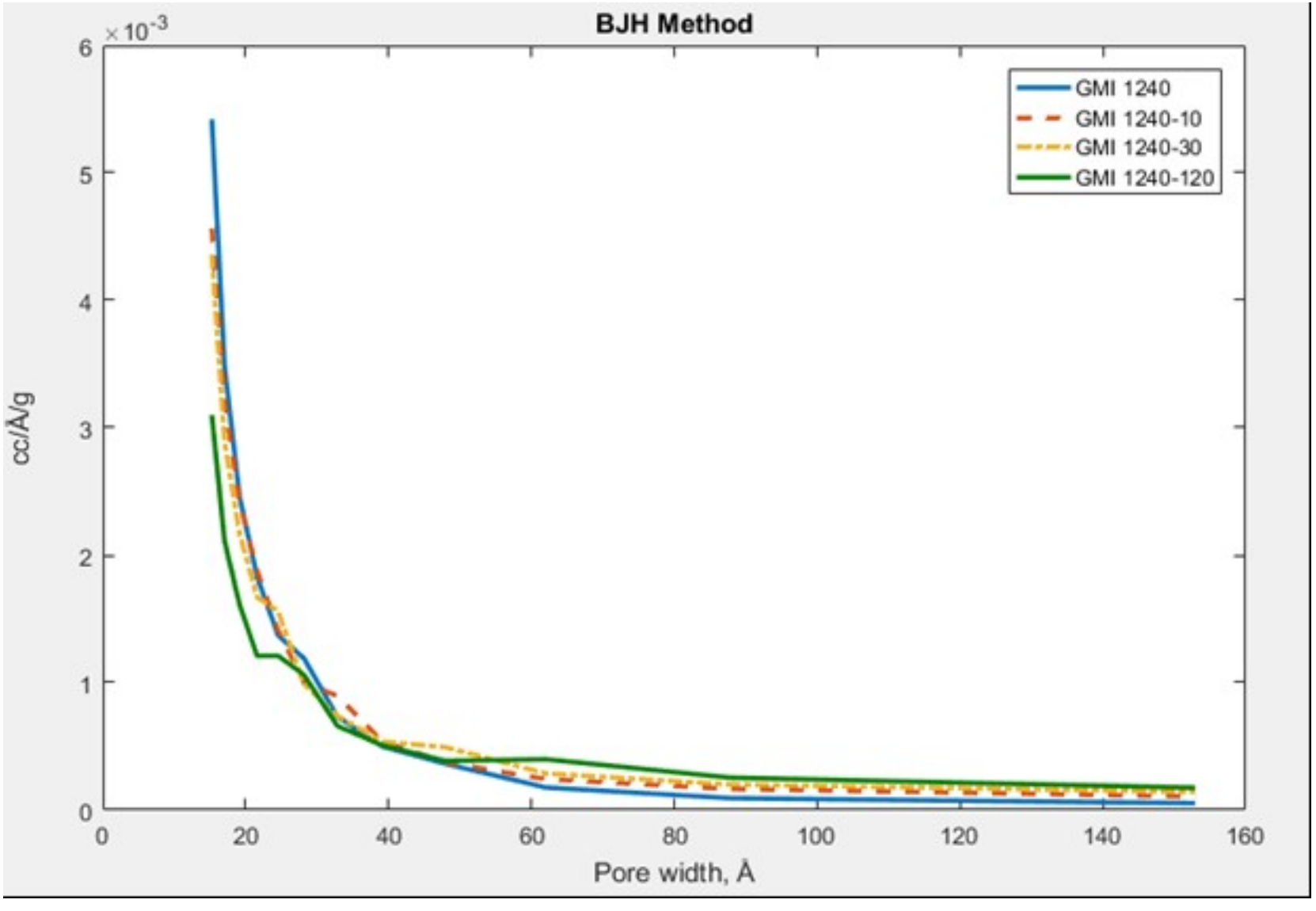
BJH Method
×10-3
6
5
4
3
2
1
0
cc/Å/g
0
20
40
60
80
100
120
140
160
Pore width, Å
GMI 1240
GMI 1240-10
GMI 1240-30
GMI 1240-120

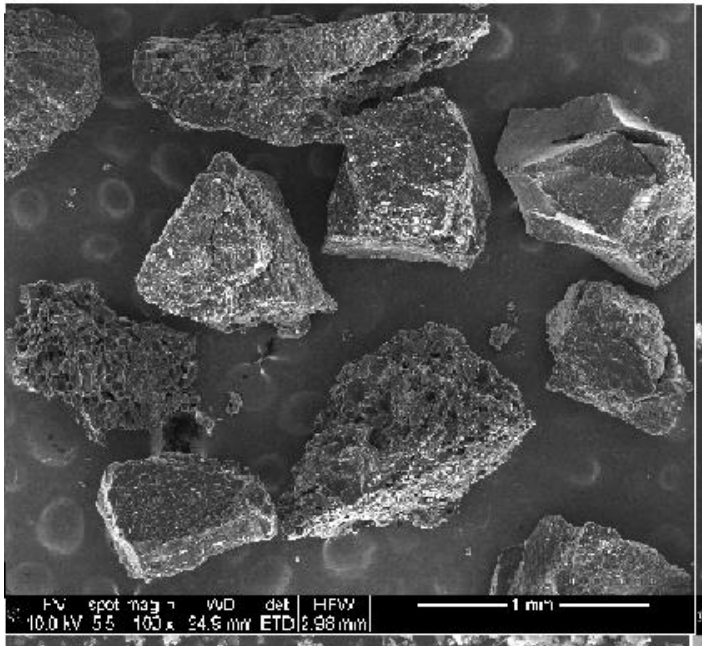
HV spot mag WD det HFW
10.0 kV 5.5 100 x 24.9 mm ETD 2.98 mm
1 mm

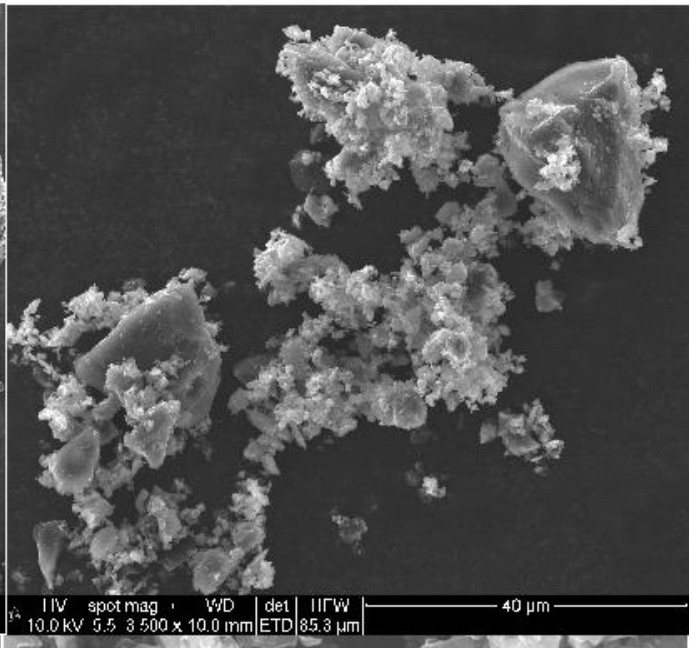
HV spot mag WD det HFW
10.0 kV 5.5 3 500 x 10.0 mm ETD 85.3 µm
40 µm

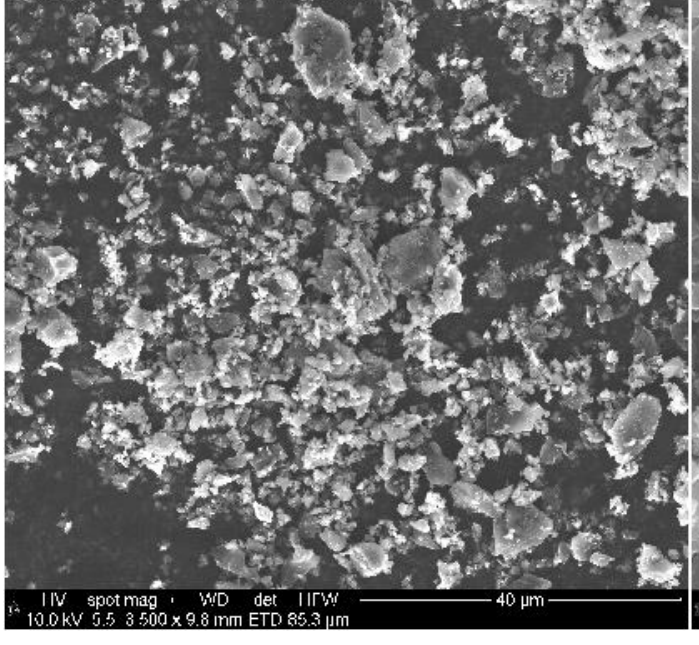
HV spot mag WD det HFW
10.0 kV 5.5 3 500 x 9.8 mm ETD 85.3 µm
40 µm

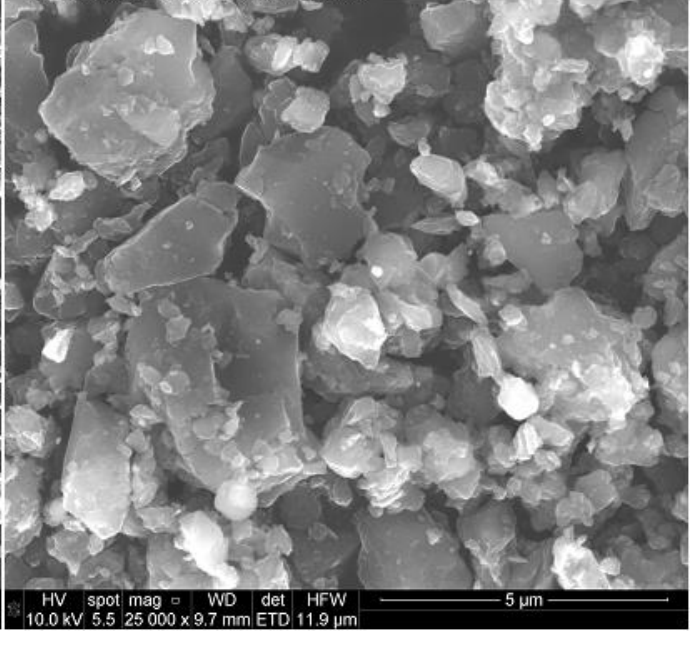
HV spot mag WD det HFW
10.0 kV 5.5 25 000 x 9.7 mm ETD 11.9 µm
5 µm

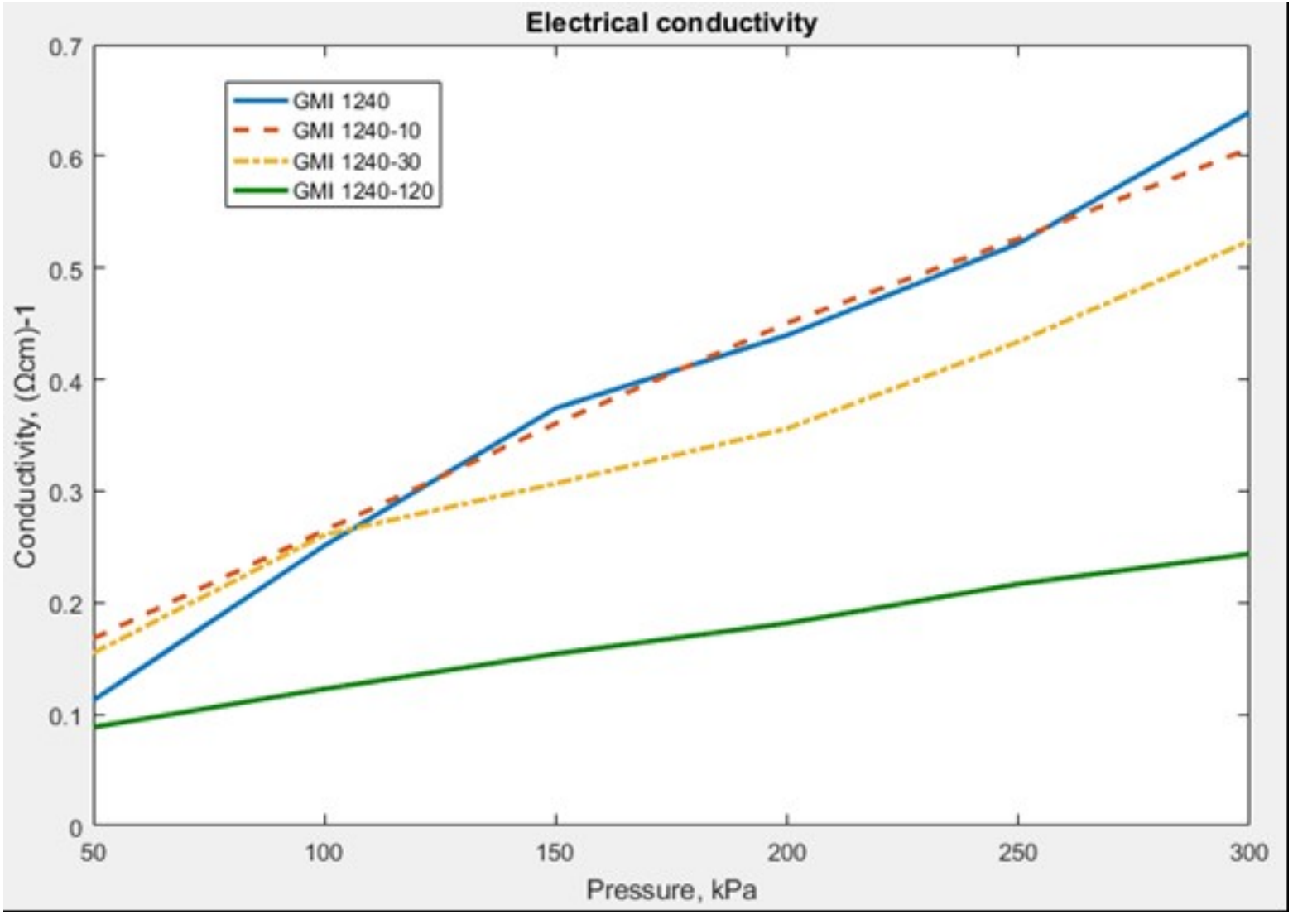
Electrical conductivity
GMI 1240
GMI 1240-10
GMI 1240-30
GMI 1240-120
Conductivity, (Ωcm)-1
Pressure, kPa
0
0.1
0.2
0.3
0.4
0.5
0.6
0.7
50
100
150
200
250
300

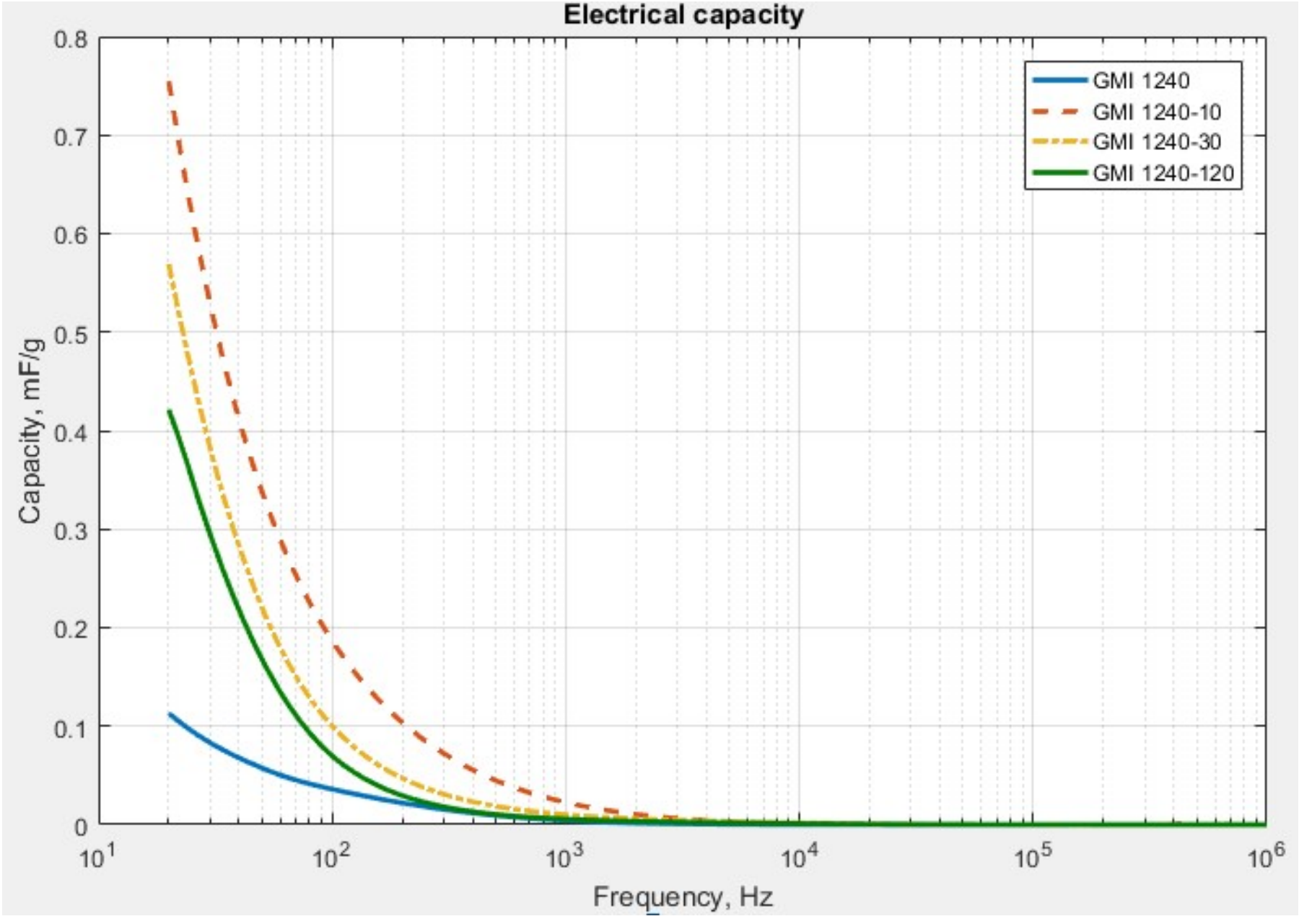
Electrical capacity
GMI 1240
GMI 1240-10
GMI 1240-30
GMI 1240-120
Capacity, mF/g
Frequency, Hz
0.8
0.7
0.6
0.5
0.4
0.3
0.2
0.1
0
10^1
10^2
10^3
10^4
10^5
10^6

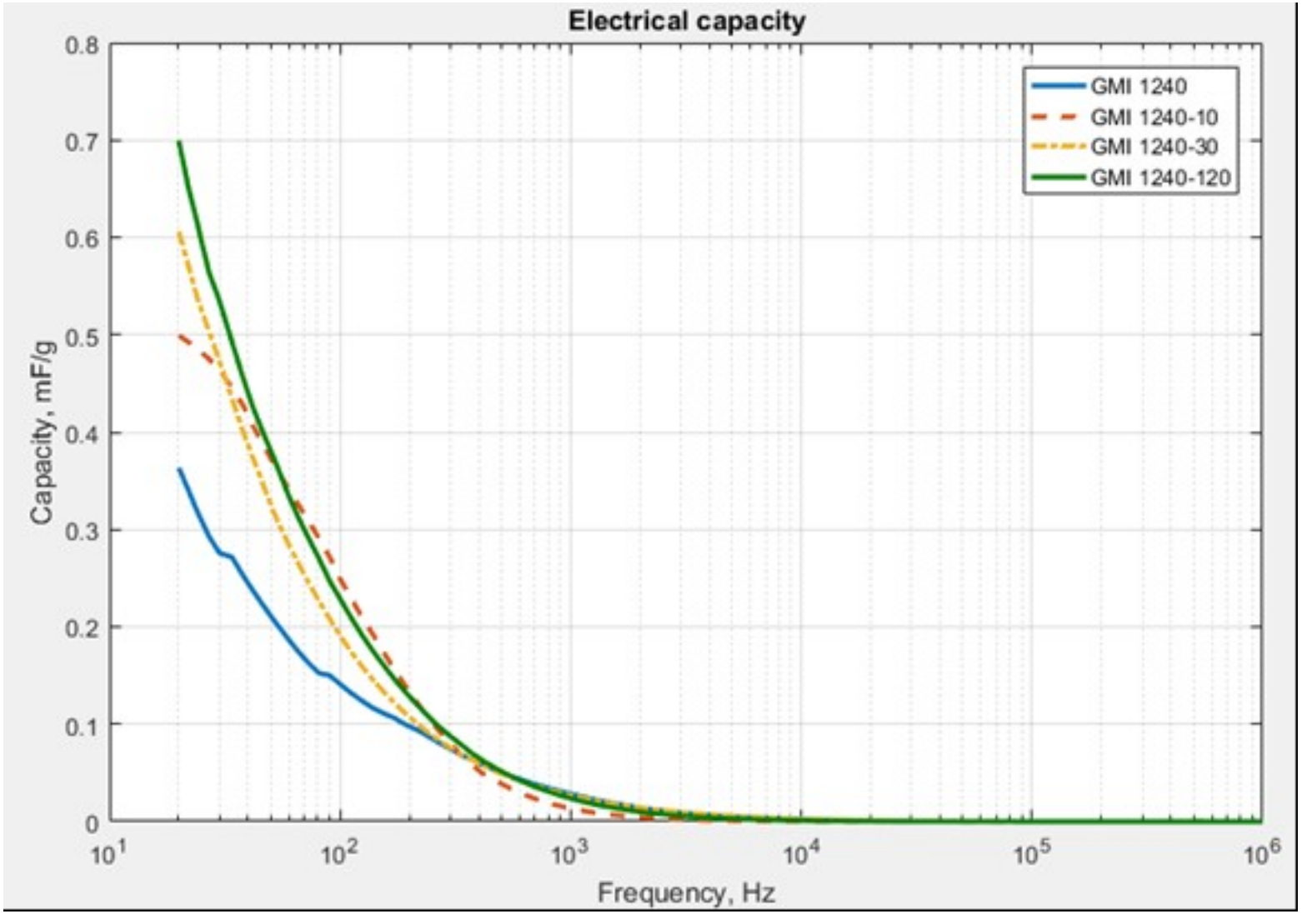
Electrical capacity
GMI 1240
GMI 1240-10
GMI 1240-30
GMI 1240-120
Capacity, mF/g
Frequency, Hz
0.8
0.7
0.6
0.5
0.4
0.3
0.2
0.1
0
10^1
10^2
10^3
10^4
10^5
10^6

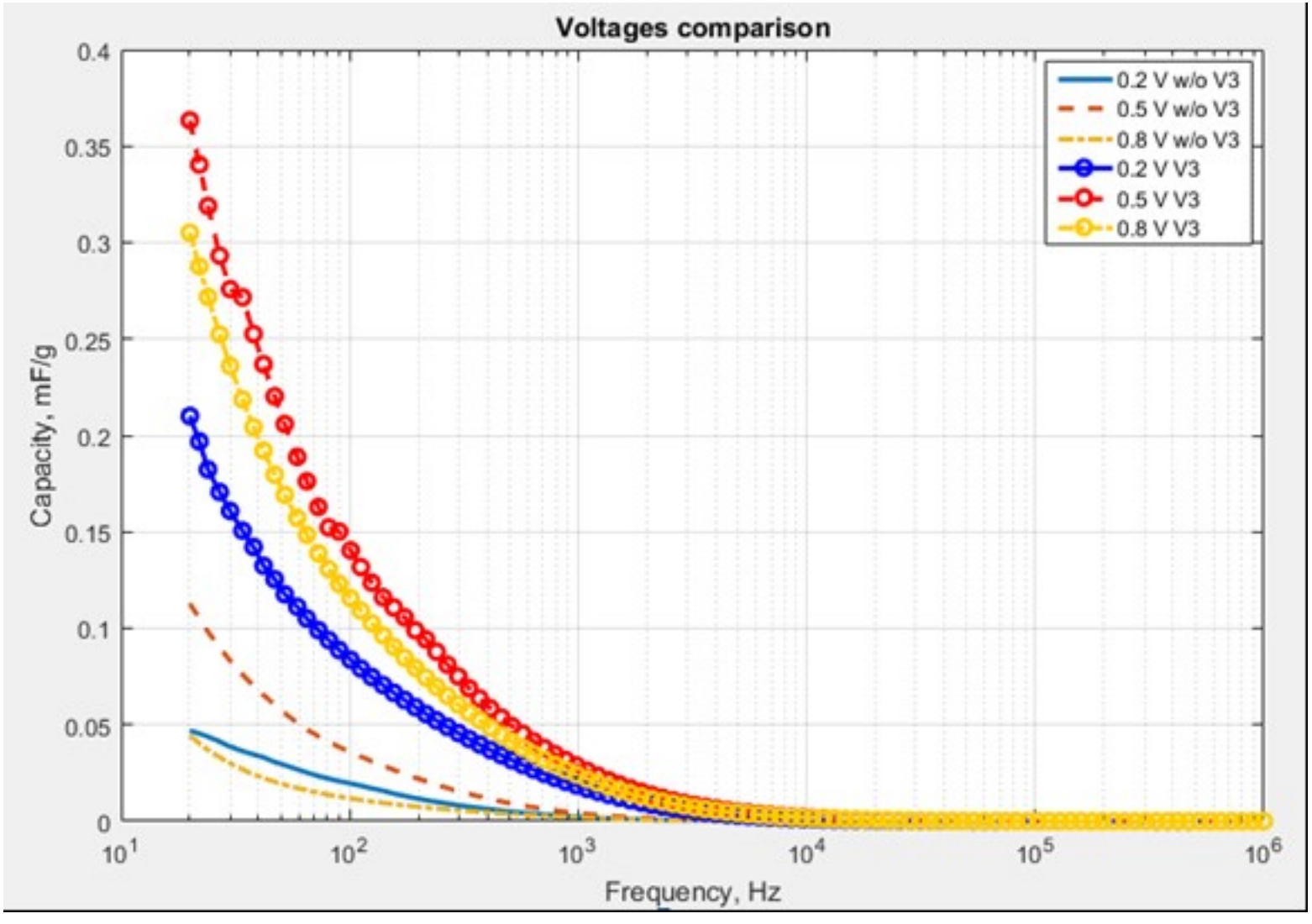
Voltages comparison
0.2 V w/o V3
0.5 V w/o V3
0.8 V w/o V3
0.2 V V3
0.5 V V3
0.8 V V3
Capacity, mF/g
Frequency, Hz
0.4
0.35
0.3
0.25
0.2
0.15
0.1
0.05
0
10^1
10^2
10^3
10^4
10^5
10^6

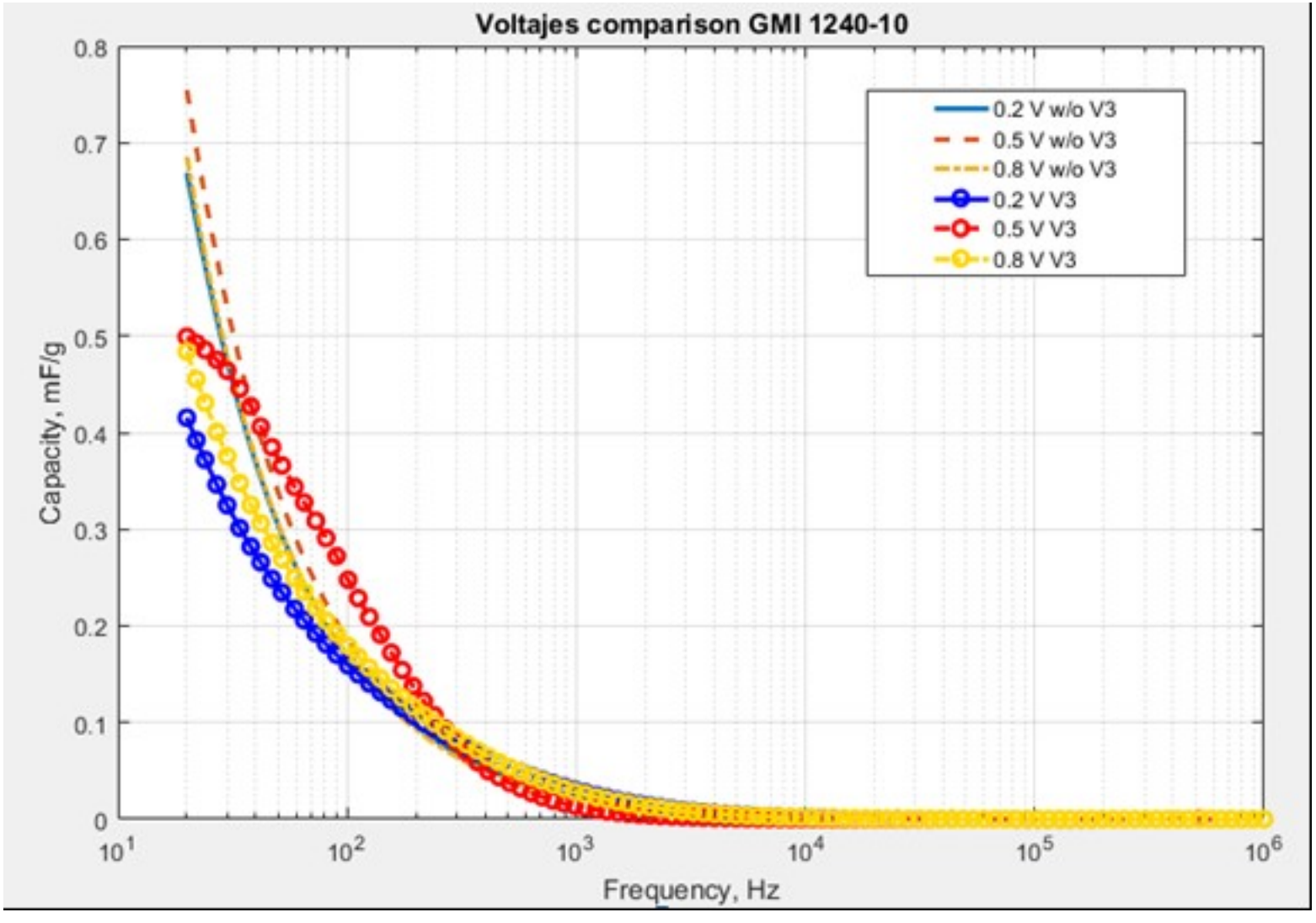
Voltajes comparison GMI 1240-10
0.8
0.7
0.6
0.5
0.4
0.3
0.2
0.1
0
Capacity, mF/g
10^1
10^2
10^3
10^4
10^5
10^6
Frequency, Hz
0.2 V w/o V3
0.5 V w/o V3
0.8 V w/o V3
0.2 V V3
0.5 V V3
0.8 V V3

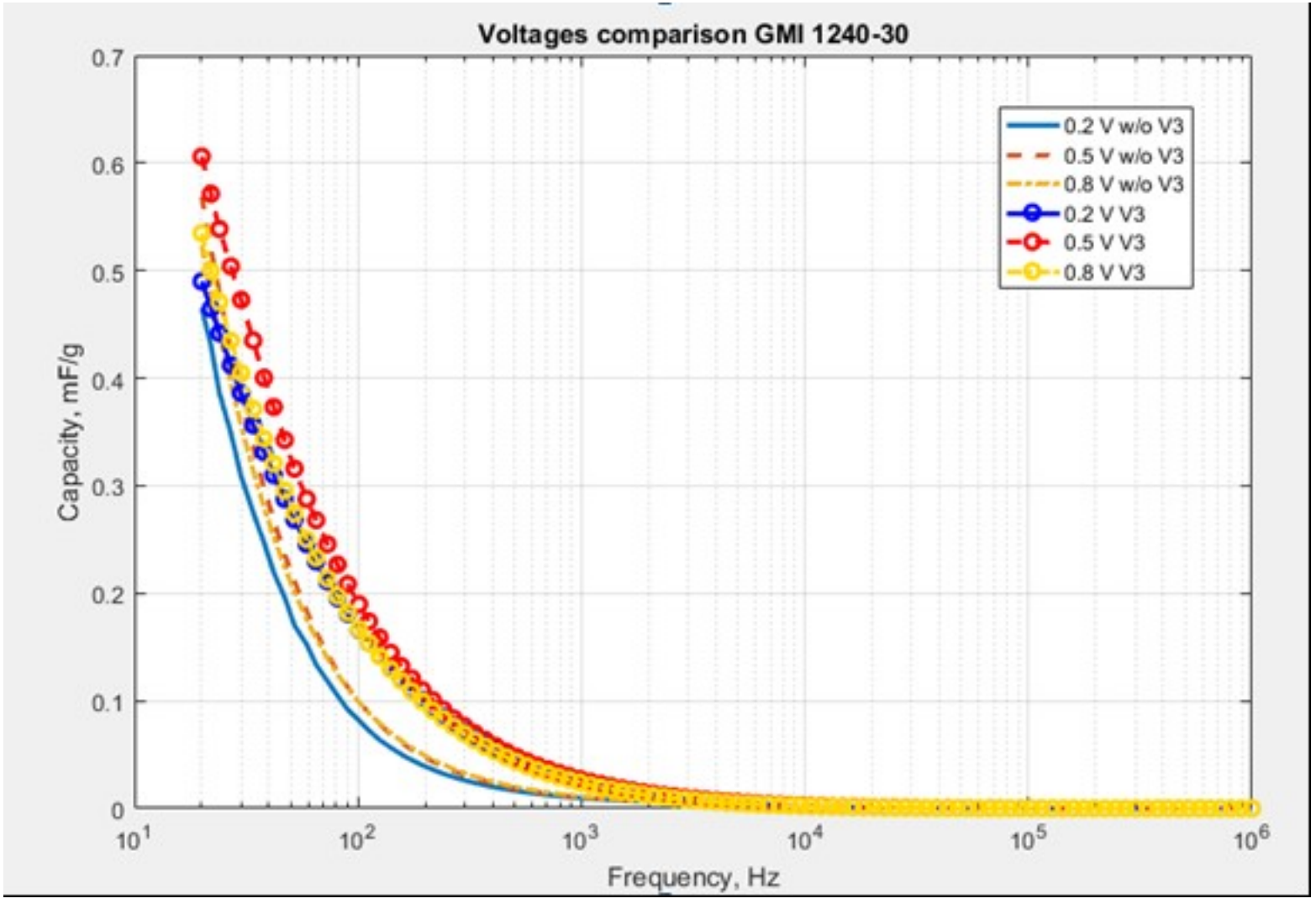
Voltages comparison GMI 1240-30
0.7
0.6
0.5
0.4
0.3
0.2
0.1
0
Capacity, mF/g
10^1
10^2
10^3
10^4
10^5
10^6
Frequency, Hz
0.2 V w/o V3
0.5 V w/o V3
0.8 V w/o V3
0.2 V V3
0.5 V V3
0.8 V V3

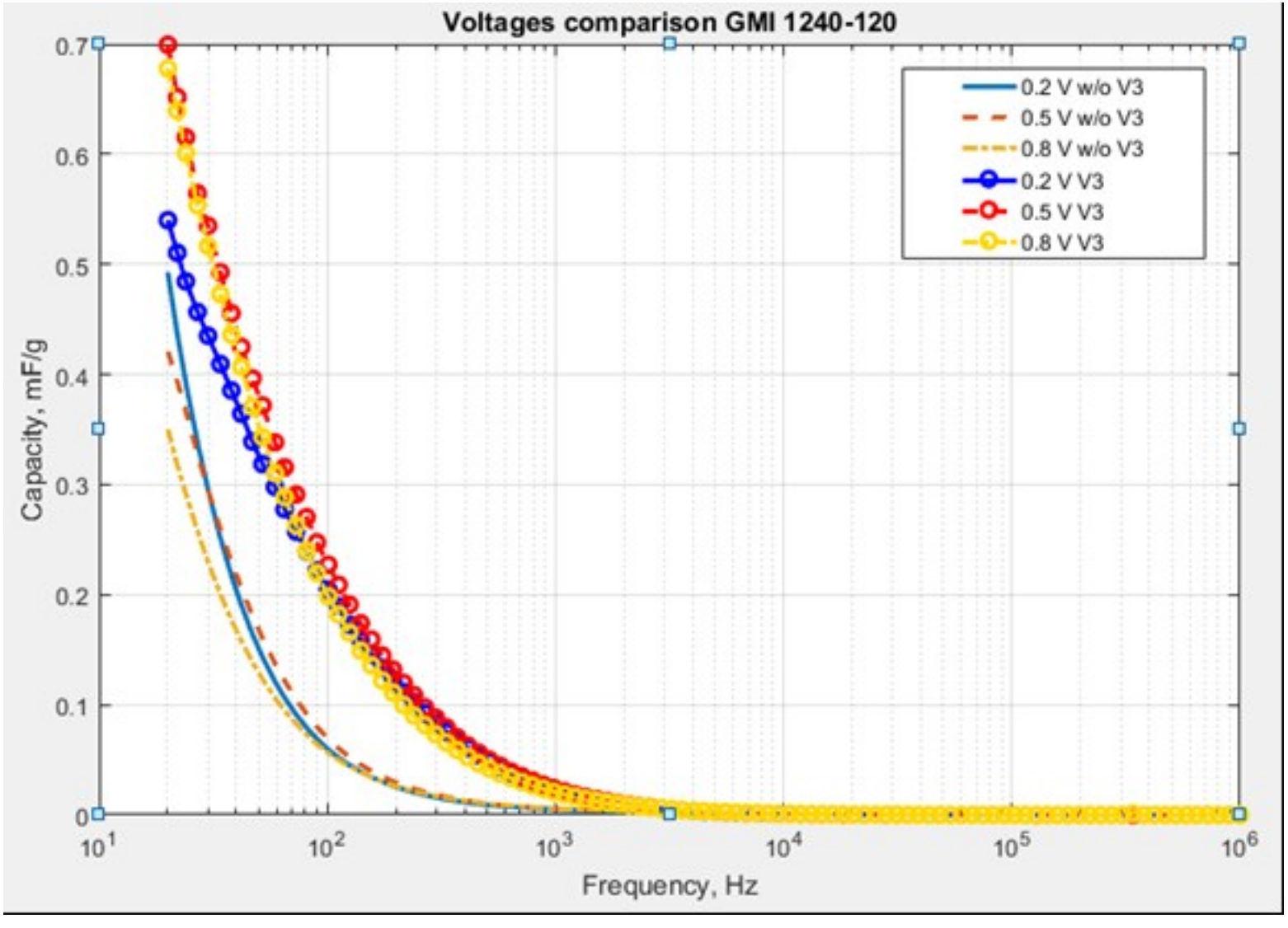
Voltages comparison GMI 1240-120
0.2 V w/o V3
0.5 V w/o V3
0.8 V w/o V3
0.2 V V3
0.5 V V3
0.8 V V3
Capacity, mF/g
Frequency, Hz
0
0.1
0.2
0.3
0.4
0.5
0.6
0.7
10^1
10^2
10^3
10^4
10^5
10^6